Reviews

Nonhydrolytic Processing of Oxide-Based Materials: Simple Routes to Control Homogeneity, Morphology, and Nanostructure

P. H. Mutin and A. Vioux*

Institut Charles Gerhardt, UMR 5253 CNRS-UM2-ENSCM-UM1, Université Montpellier 2, cc 1701, Place Eugène Bataillon, 34095 Montpellier cedex 5, France

Received August 31, 2008. Revised Manuscript Received November 14, 2008

Over the past decade, there has been an increasing number of reports on low-temperature preparations of oxides and organic–inorganic hybrids (including sol–gel, solvothermal synthesis, and atomic layer deposition) that take place in nonaqueous media and involve no water as a reactant. This growing interest lies on the ability of these nonhydrolytic routes (in organic solvents, unusual media, condensed phase or under vapor deposition conditions) to reach a higher control over composition, morphology, and structure. An overview of the main results is proposed here, which emphasizes the molecular approach (molecular precursors used, nonhydrolytic reactions involved), the ability to design oxide-based materials with a high degree of homogeneity (mixed oxides, organically modified silicates and ceramics, polysiloxane resins, polymer nanocomposites, etc.) and specific nanostructures (nanoparticles, mesocrystals, nanoporous materials, nanocomposites, nanolayers).

1. Introduction

The low-temperature formation of oxo bridges by condensation of molecular precursors holds a significant place in materials chemistry as a versatile way of synthesizing oxides and hybrid organic–inorganic materials, either by inorganic polymerization processes (precipitation and sol–gel methods, associated or not with hydrothermal treatments) or by surface modification of the hydroxylated surface of inorganic substrates.

The versatility in shaping offered by sol–gel synthesis make it particularly adapted to the processing of advanced materials: thin films, self-standing membranes, nanoparticles with controlled size, etc. During the last 15 years, there has been a massive amount of research in hydrothermal and sol–gel chemistry for the control of the texture of inorganic matter using organic matter as templates, opening access to hierarchical structures. Moreover, combined with macromolecular chemistry, sol–gel chemistry leads to nanocomposites, including polymers reinforced with inorganic nanofillers, inorganic nanoparticles coated with an organic layer, and biphasic systems with two interpenetrating continuous phases, opening access to unique functional materials. In nanocomposites, the decisive effects of interface bonding through coupling agents emphasize the importance of surface condensation reactions, which generally involve surface hydroxyl groups and adsorbed water molecules.

Most often the formation of oxo bridges takes place at low temperatures in aqueous or aquo-organic media. Actually, the formation of oxo-bridges involves successively hydrolysis and condensation reactions occurring as separate or overlapping steps, which results in different nucleation-growth processes. Moreover, hydrolysis and condensation reaction rates are often too fast, especially with transition metal precursors, making it uneasy to control the processes. This can be a major downside in low-temperature processes where slight changes in kinetics may result in drastic changes in the structure, the texture, and the morphology of the final materials.

The desire to explore alternative low-temperature reactions has prompted growing interest in nonhydrolytic ways during the last 15 years. The scope of the present review covers the preparation of oxide and hybrid organic–inorganic materials based on nonhydrolytic (NH) condensation reactions, that is, condensation reactions in which oxo bridges originate from oxygen-donors other than water.

NH condensations can be carried out in solution in organic solvents or in unusual media as melt polymers, ionic liquids, supercritical fluids, etc., as well as in the gas phase. Accordingly, beyond solvothermal and sol–gel syntheses, NH condensations concern thermal decomposition methods, atomic layer deposition (ALD), as well as surface modification.

Comprehensive reviews have already been published on nonhydrolytic sol–gel routes[1] applied to the preparation of oxides,[2] organic–inorganic hybrids,[3,4] metal oxide nanoparticles,[5–11] and nanomaterials.[12] This review aims at outlining the basic chemical reactions involved in NH syntheses and the main applications reported, especially in the most recent period, in the field of mixed-oxide materials and organic–inorganic hybrids, with a special stress on nanostructuration

---

* Corresponding author. E-mail: vioux@univ-montp2.fr.

10.1021/cm802348c CCC: $40.75

aspects (nanoparticles, porous materials, thin films, monolayers, nanocomposites, etc.).

2. Nonhydrolytic Condensation Reactions

The oxide bridge formation by condensation reactions is regarded as nonhydrolytic when the oxygen donor is not water. Such reactions may take place in organic solvents, condensed phase, or under vapor deposition conditions. Condensation reactions that do not involve any hydroxyl groups (namely aprotic condensations) are strictly NH. So are the reactions that involve hydroxyl groups as far as the formation of water by M−OH self-condensation is prevented by kinetics. Reactions which involve the in situ generation of water cannot be regarded as strictly NH. However, some nonstrictly NH reactions that are of particular interest for processing in nonaqueous media will be mentioned here as "borderline" cases.

Nonhydrolytic processes may be classified according to the nature of the metal precursor (halide, alkoxide, acetylacetonate etc.), the nature of the oxygen donor (alkoxide, alcohol, ether, etc.) or the nature of the predominant molecule eliminated (alkyl halide, ether, ester, etc.). The latter classification appears more informative on the process by associating it to a specific NH reaction pathway, even though generally several molecules may be released in a process, in relation to successive or competitive reactions.[13] In this part, we give an overview of the main low-temperature aprotic condensation reactions and NH hydroxylation reactions, followed by a glance on thermal decomposition reactions.

2.1. Alkyl Halide Elimination. Early explored by Gerrard in the 1950s,[14] NH condensations involving the elimination of alkyl halide between metal alkoxides and metal halides (most often chlorides) (eq 1) were introduced in sol−gel chemistry in the 1990s,[15,16] before becoming one of the most widely used nonhydrolytic pathways

$$\text{M-Cl} + \text{M-OR} \rightarrow \text{M-O-M} + \text{R-Cl} \qquad (1)$$

In the case of metals and transition metals, this reaction takes place around 100 °C using simple primary or secondary R groups, bringing out higher activation energies than hydrolytic processes. The reactivity is even lower in the case of silicon, and elimination of alkyl chloride requires tertiary alkyl or benzylic R groups.[17] Otherwise, with primary or secondary R groups, a Lewis acid catalyst, such as $FeCl_3$ or $AlCl_3$, is needed to catalyze the condensation.[18]

In the preparation of silicates SiO_2-MO_n (M = Ti, Zr, Al, etc.), the reactivities of silicon and metal precursors are leveled, the metal species acting as Lewis acid catalyst.[19] As a consequence, this NH condensation route turned out to be particularly interesting for the preparation of homogeneous silicates SiO_2-MO_n.

Alternatively the alkoxide groups can be formed in situ by reaction of halide groups with an organic ether (eq 2) or an alcohol (eq 3), which is of particular interest if the alkoxide is expensive or is not commercially available

$$\text{M-Cl} + \text{ROR} \rightarrow \text{M-OR} + \text{R-Cl} \qquad (2)$$

$$\text{M-Cl} + \text{ROH} \rightarrow \text{M-OR} + \text{H-Cl} \qquad (3)$$

Thus, three different ways can be used to form oxo bridges, involving the reaction of metal (or silicon) chlorides with either alkoxides, ethers or alcohols as oxygen donors. In all cases the alkyl halide formation results from a nucleophilic substitution at the carbon center, involving $(MO)^{\delta-}R^{\delta+}$ polarization, rather than $M^{\delta+}(OR)^{\delta-}$ polarization. Accordingly, the alkyl halide elimination route can be applied to a wide range of metals, a part from alkaline and alkaline earth metals, and any electronic effect favoring the formation of a carbocation will facilitate the condensation reaction.

Note that in the reaction with alcohol (eq 3), the HCl formed may catalyze secondary reactions, such as ether elimination (see below) leading to complex pathways. In addition, depending on the nature of the alcohol, nonhydrolytic hydroxylation with elimination of alkyl chloride may occur, as reported for the reaction of $SiCl_4$ with tertiary or benzylic alcohols[20] (eq 4)

$$\text{M-Cl} + \text{ROH} \rightarrow \text{M-OH} + \text{R-Cl} \qquad (4)$$

2.2. Ether Elimination. Ether elimination between alkoxide groups (eq 5) has been postulated in the formation of metal oxoalkoxides from alkoxides (especially rhenium, molybdenum and to a lesser extent tungsten alkoxides).[21] It requires relatively high temperature and has been noticed in thermal decomposition rather than sol−gel processing.

$$\text{M-OR} + \text{M-OR} \rightarrow \text{M-O-M} + \text{R-O-R} \qquad (5)$$

However, in the synthesis of methoxylated silicone resins by reaction between $Si(OMe)_4$ and Me_2SiCl_2, significant Me_2O elimination occurred, in addition to MeCl, depending on the nature of the Lewis acid catalyst.[22]

Similarly, in the reaction between metal halides and alcohols, the release of ethers (dehydration of alcohol) was observed besides alkyl halides in varying amounts depending on the system; the formation of ether was even the major reaction under solvothermal conditions (in autoclave at 100−160 °C).[23] Benzyl alcohol is known to favor ether elimination.[8] Stucky et al. reported the synthesis of nanoparticles of various metal oxides from the reaction of metal chlorides (or oxychlorides) with benzyl alcohol. The process led to highly crystalline nanoparticules at relatively low temperature (typically between 40 and 175 °C) and was further extended by Niederberger et al. to other metals.[24] The release of dibenzylether was clearly evidenced in the case of HfO_2.[25]

It is worth mentioning here the NH condensation involving the release of thioether from chlorosilanes and DMSO[26] according to

$$SiCl_4 + 2CH_3S(O)CH_3 \rightarrow SiO_2 + 2ClCH_2SCH_3 + 2HCl \qquad (6)$$

2.3. Ester Elimination. Direct NH condensation between metal carboxylates $M(OCOR)_x$ and metal alkoxides $M'(OR')_y$ (eq 7) in nonpolar, aprotic solvents has been proposed as a general nonhydrolytic sol−gel route to metal oxides.[27,28]

$$\text{M-OR}^1 + \text{M-OCOR}^2 \rightarrow \text{M-O-M} + \text{R}^2\text{COOR}^1 \qquad (7)$$

The reaction of alkoxide precursors with carboxylic acids offers an alternative sol−gel route in nonaqueous solvents. The first step of the process is the liberation of alcohol

Scheme 1

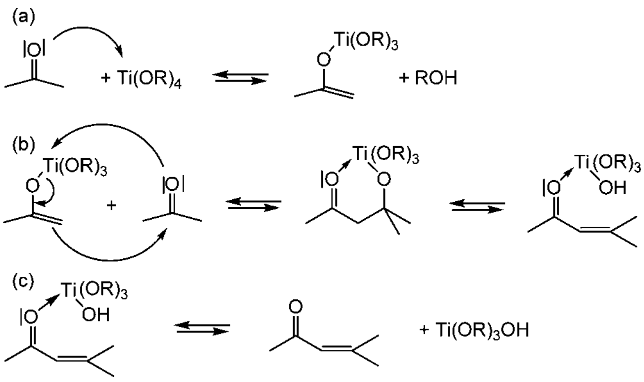

Scheme 2

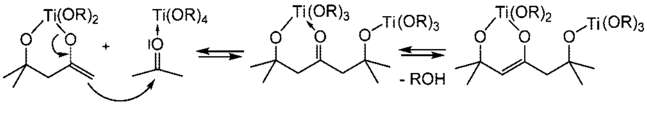

molecules by the exchange of carboxylate and alkoxy groups on the silicon or metal atom (eq 8).[29]

$$M(OR^1)_n + R^2COOH \rightarrow M(OR^1)_{n-1}(OCOR^2) + R^1OH \quad (8)$$

Although direct aprotic condensation (eq 7) cannot be ruled out in all cases, the nonhydrolytic hydroxylation of carboxylate derivatives (e.g., acetoxysilane) by the nascent alcohol (eq 9)[29] is most likely to occur, as well as the esterification of carboxylic acid (eq 10) with in situ generation of water,[30] which makes this process non strictly nonhydrolytic, at least in solution. On the other hand, this reaction has been used recently for the vapor phase deposition of metal oxides[31] (see section 4.3.1). On the basis of kinetic considerations, the authors conclude to a pathway involving mainly acetoxylation (eq 8) followed by aprotic condensation (eq 7). In this case, the alcohol formed in the first step is likely removed in the vapor phase and cannot react on the surface with the carboxylic acid to form ester and water (eq 10).

$$M(OR^1)_{n-1}(OCOR^2) + R^1OH \rightarrow M(OR^1)_{n-1}(OH) + R^2COOR^1 \quad (9)$$

$$R^1OH + R^2COOH \rightarrow R^2COOR^1 + H_2O \quad (10)$$

Formic acid[32,33] as well as acetic acid[29,34,35] were successfully used for synthesizing silica and hybrid materials. The reaction of alkoxide precursors with carboxylic acids is particularly interesting with high-molecular-weight silane precursors with limited solubility in water–alcohol mixtures, such as star alkoxysilane molecules,[36] or when performing sol–gel synthesis in unusual media, such as perfluoro solvents,[33] ionic liquids,[37,38] and supercritical CO_2.[39] It is noteworthy that hybrid organic–inorganic gels were prepared by this way, in which the silica-like domains bearing the organic groups (e.g., amino groups) were found to be luminescent centers.[35,40] Mesoporous TiO_2 nanofibers and ZrO_2 aerogels were recently synthesized by reacting metal alkoxides and acetic acid in supercritical CO_2.[41,42]

Alternatively, the reaction of metal or silicon alkoxides with acid anhydride (eq 11) leads to the in situ formation of carboxylate groups, which can then condense with alkoxide groups (eq 7), providing an unambiguously nonhydrolytic (and hydroxyl-free) sol–gel route.

$$M(OR^1)_n + (R^2CO)_2O \rightarrow M(OR^1)_{n-1}(OCOR^2) + R^2COOR^1 \quad (11)$$

This route was successfully used to prepare titania (in the presence of $TiCl_4$ catalyst)[43] and silica–titania mixed oxides.[44]

The preparation of nanoscaled TiO_2 powders with narrow size dispersion from titanium isopropoxide and acetic or trifluoroacetic anhydrides in supercritical CO_2 was recently reported.[45] Interestingly, the NH condensation of tetraethoxysilane with acetic anhydride was shown to be catalyzed by titanium tetra(trimethylsiloxide) at high temperature, leading to hyperbranched polyalkoxysiloxanes.[46]

2.4. Amide Elimination. Another NH hydroxylation reaction is provided by the amide elimination of carboxylated precursors (eq 12).

$$M(OR^1)_{n-1}(OCOR^2) + R^3NH_2 \rightarrow M(OR^1)_{n-1}(OH) + R^2CONHR^3 \quad (12)$$

This aminolysis route has been used to give monodisperse TiO_2 nanorods with controlled length.[47] The synthesis of ZnO nanocrystals by reacting zinc acetate with alkylamines at 220–300 °C in the presence of *tert*-butylphosphonic acid as a capping agent could involve the same NH hydroxylation reaction.[48]

2.5. Elimination of α,β-Unsaturated Carbonyl Compounds and Related Compounds through the Formation of Enolates. As esterification and alcohol dehydration, aldol condensation is able to generate water, through the subsequent formation of α,*β*-unsaturated carbonyl compounds (crotonization reaction; eq 13).

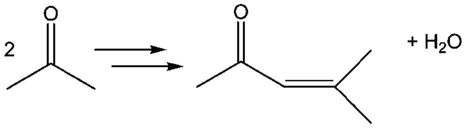

However, as in esterification and alcohol dehydration reactions, the elimination of water may be regarded as only formal in the presence of a large amount of Lewis acid metal centers (metal complexes or/and incipient metal oxide colloids), as shown in Scheme 1 where only M–OH groups are eliminated (NH hydroxylation reaction). Accordingly, ketones or aldehydes can be used as oxygen donors in nonhydrolytic processes. Sanchez et al. prepared well-defined titanium oxo-clusters by reacting titanium isopropoxide with acetone, acetylacetone and diacetone alcohol at room temperature.[49,50] Niederberger et al. reported that in ketones and aldehydes under solvothermal conditions highly crystalline anatase nanoparticles were obtained (typically 5–20 nm in acetone at 130 °C).[51] Both groups also detected products stemming from further condensation reactions, as illustrated in Scheme 2, whereas Meerwein–Ponndorf–Verley reduction of the ketone to alcohol could contribute to increase the number of byproduct, especially in benzaldehyde.[51]

Scheme 3

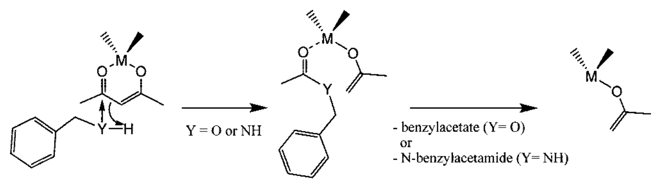

Scheme 4

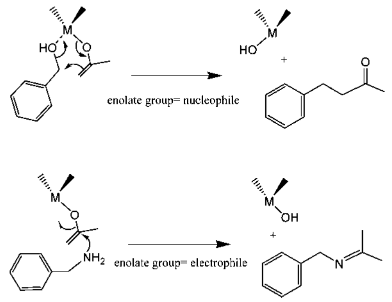

Scheme 5

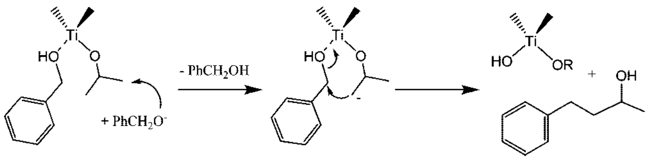

Scheme 6

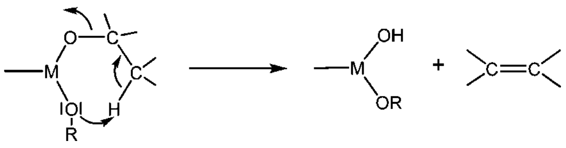

In these processes, titanium enolates are the key intermediates. It is worth noting that metal acetylacetonates, which may be more available than alkoxides for some metals, have been shown to be able to release enolate derivatives on heating in benzyl alcohol and benzyl amine. Actually they can be used as oxide precursors through complex reaction pathways involving enolate formation (C−C bond cleavage, Scheme 3), followed by condensation reactions (C−C bond formation, Scheme 4).[8] Solvothermal reactions of metal acetylacetonates in benzyl alcohol and benzylamine were shown successful in the preparation of oxide nanoparticles (see below).[52−54]

2.6. Alcohol Elimination Involving C−C Bond Formation. In benzyl alcohol and its derivatives, metal alkoxides may undergo a different reaction from the above-mentioned etherification under specific conditions, such as the presence of basic species. The preparation of perovskite nanoparticles ($BaTiO_3$, $SrTiO_3$, $(Ba,Sr)TiO_3$, and $LiNbO_3$) has been recently developed via a simple one-pot reaction process involving the dissolution of elemental alkali or alkaline earth metals in benzyl alcohol before the addition of titanium tetraalkoxide.[55,56] The major formation of 4-phenyl-2-butanol and 1,5-diphenyl-3-pentanol gave evidence of a reaction involving C−C bond formation between benzyl alcohol and the isopropanolate ligand (Scheme 5).[8]

Related reaction pathways were reported for vanadium isopropoxide oxide and niobium ethoxide,[57] and for yttrium isopropoxide.[58] Yttrium oxide was shown to further catalyze hydride-transfer reactions (namely Oppenauer reactions, i.e., reverse Meerwein−Ponndorf−Verley reactions) to form benzoic acid and toluene from benzyl alcohol via benzaldehyde.

2.7. NH Condensations Involving Hydroxyl Groups: Elimination of H−X. As illustrated above, condensation reactions involving hydroxyl groups can be considered strictly NH as far as self-condensation does not lead to the formation of water. This is the case when a controlled NH process provides hydroxyl groups that undergo in situ cross-condensation reactions in the presence of a large amount of reactive groups (eq 14)

$$M{-}OH + M{-}X \rightarrow M{-}O{-}M + H{-}X \qquad (14)$$

where X = H, Cl, NR_2, OR, OCOR, acac, $OSi(OR)_3$, etc.

It is worth mentioning that this is also the case with relatively stable hydroxyl groups, as B−OH,[59] P−OH, [60] sterically hindered Si−OH,[61−63] and surface hydroxyl groups on inorganic supports.[64,65] The same pathway probably occurs in most syntheses involving the thermal decomposition of precursors under dry conditions (see below).

2.8. Thermal Decomposition. Generally speaking, when the reaction temperature increases the reaction pathways become more and more complex, which is expected if one keeps in mind that precursors, intermediate compounds and oxide products are able to act as catalysts in numerous by-reactions such as dehydrohalogenation, polymerization, oxidation, etc. Another general feature of high-temperature processes is the thermal decomposition of precursors.

Thus, decomposition of alkoxide precursors generally involves alkene elimination and formation of hydroxyl groups, as observed, for instance, in the preparation of silica-modified titania by pyrolysis at 300 °C of titanium and silicon alkoxides (Scheme 6).[66] Propene, along with propyl chloride, has also been detected in the atomic layer deposition at 165 °C of $Zr_xTi_yO_z$ films by alternate pulsing of $ZrCl_4$ and $Ti(O^iPr)_4$ on a silicon substrate.[67]

The thermolysis, at relatively mild temperatures (100−180 °C), of tri*tert*-butoxysiloxy derivatives $M(OSi(O^tBu)_3)_n$ has been used to prepare mixed metal oxides.[68−72] However, this reaction cannot be considered strictly NH, as it involves the elimination of both isobutylene and water.

3. Control of the Composition and Homogeneity of Materials by Using NH Condensation Reactions

NH condensation reactions feature more controllable kinetics than hydrolysis−condensation ones, as they involve higher activation energy. Accordingly, they provide simple routes to single-phase mixed oxides and highly homogeneous hybrid materials in some cases where aqueous routes are made difficult by the different reactivity of the molecular precursors. Moreover in hybrid organic−inorganic systems, they combine the advantage of a better miscibility of the organic components by using nonaqueous media.

3.1. Mixed Oxides. NH routes, especially those based on the elimination of alkyl halide (eqs 1−3), were shown to provide an excellent control over stoichiometry and homogeneity in mixed oxides. This has been illustrated in many binary oxide systems, including Si−Ti,[19,73,74] Si−Zr,[19] Si−Al,[73,75−77] Sn−Al,[78] Ti−Al[79−81] Ti−Zr,[82,83] Zr−Mo,[84] Ga−Mo,[85] V−Nb,[86] Fe−Ti,[87] and Ti−V.[88,89] The same method was also applied to some ternary systems, such as V−Si−Nb,[86] Co−Al−Si,[90] and even to quaternary NASICON system ($Na_3Zr_2Si_2PO_{12}$).[91]

The excellent molecular scale homogeneity of NH xerogels may result in the formation of metastable phases on annealing. Thus, NH mixed oxides prepared by the alkoxide route (eq 1) with an Al/Ti ratio of 2 directly crystallized into metastable pseudobrookite β-$TiAl_2O_5$, rather than into the stable rutile and corundum phases.[79] This behavior reflects that starting from a homogeneous gel, the crystallization of the metastable mixed oxide requires shorter-range diffusion of atoms than the phase separation to the stable phases and is thus significantly faster.

The syntheses of some other metastable phases were reported by the ether route (eq 2), as the new zirconium tungstate and gallium molybdate polymorphs, ZrW_2O_8 (structurally related to trigonal $ZrMo_2O_8$)[84] and $Ga_2Mo_3O_{12}$ (monoclinic $Sc_2W_3O_{12}$ structure).[85]

Several of these NH mixed oxides have been successfully tested as catalysts and catalyst supports: Nb−V(-M) (M = Mo, Sb, Si) and Sb−V in the oxidative dehydrogenation of propane,[86,92,93] Si−Ti in the epoxidation of alkenes with alkylhydroperoxides[94,95] and in the oxidation of sulfur compounds with hydrogen peroxide,[96] V−Ti in the selective catalytic reduction of NO_x by NH_3,[88,89] Co−Al−Si in the selective oxidation of (*Z*)-cyclooctene, cyclohexane, and *n*-heptane by iodosylbenzene.[90] The high catalytic activity of NH Si−Ti mixed oxides in oxidation reactions has been shown to be related to the high dispersion of Ti sites in the silica network, the NH route preventing the formation of TiO_2 domains.[95−97] Conversely, the activity of V−Ti catalysts resulted from the migration of V species from the bulk to the surface during the calcination at 500 °C of V−Ti xerogels, made possible by the rather low Tammann temperature (the temperature at which bulk atoms exhibit mobility) of vanadia (481 K).[89]

The high H_2O_2 selectivity of NH Si−Ti catalysts in the oxidation of sulfur compounds with hydrogen peroxide,[96] has been ascribed to the low density of silanols in the calcined xerogels (in comparison to Ti-MCM 41) resulting from a high degree of condensation.

Mixed-oxides prepared by thermal decomposition of terbutoxysiloxy derivatives (see above) have also been evaluated as catalysts for various oxidation reactions,[72,98,99] although the grafting of silica surfaces by these derivatives afforded more efficient catalysts.[65,100]

3.2. Organic−Inorganic Hybrid Materials. Although the reaction conditions (temperature, presence of Lewis acid species) are less mild than in conventional hydrolytic sol−gel, NH routes can be used for the encapsulation or the covalent immobilization of organic or organometallic species in oxide matrices. More widely, NH routes were successfully applied to all classes of organic−inorganic hybrid materials (including polysiloxane resins, organically modified silicates and ceramics, and polymer nanocomposites),[3] as they allow us to circumvent such impediments as the poor solubility of most organic components in water-containing systems, phase separation between organic and inorganic components, use of only hydrosoluble polymers, etc.

3.2.1. Encapsulation of Organics. Hybrid catalysts have been prepared by successful encapsulation of metal complexes (metalloporphyrins, tetraazaannulenato nickel complex, Jacobsen catalyst) in amorphous alumina matrices prepared by condensation of $AlCl_3$ with diisopropyl ether (eq 2).[101−103] These works underline the advantage of the NH route in making catalyst sites more active, avoiding their destruction as well as the formation of dimeric species.

3.2.2. Polysiloxane Resins. Homogeneous polysiloxane resins incorporating both $Me_2SiO_{2/2}$ (D) and $SiO_{4/2}$ (Q) units are not easily prepared by conventional hydrolytic way, due to the large difference of reactivity between difunctional and tetrafunctional monomers. However, methoxylated polysiloxane D/Q resins with a high content of Q units were prepared by the solvent-free, nonhydrolytic condensation between Me_2SiCl_2 and $Si(OMe)_4$ at 130 °C in the presence of 1 mol % $ZrCl_4$ catalyst[22] (eq 1). These liquid resins, which could be cured by ambient humidity after application, consisted in a complicated mixture of oligomers, linear or branched ($n > 1$) and cyclic ($n > 3$), with a high degree of D/Q bonding. The distribution of Si-OMe and Si-OSi bonds and the bonding between D and Q units were found to be purely random. This was ascribed to the occurrence of Si-OSi/Si-OMe and Si-OSi/Si-OSi redistribution reactions that reached equilibrium in the liquid state (thus, thermodynamic control would account for the homogeneity in the case of polysiloxane resins, whereas kinetic control would account for the homogeneity in the case of the above-mentioned metastable mixed oxide gels). The significance of Si-OSi /Si-OSi redistributions was also evidenced by the nonhydrolytic preparation of highly homogeneous D/Q resins from $SiCl_4$, tetraalkoxysilane, and octamethylcyclotetrasiloxane (D_4) in the presence of $ZrCl_4$ catalyst,[22] or hexamethylcyclotrisiloxane (D_3) in the presence of $FeCl_3$.[104] The solvent-free nonhydrolytic preparation of polysiloxane resins built up of both $SiO_{4/2}$ (Q) and $RSiO_{1.5}$ (T) units was also reported.[105]

Hydroxyl-free organosilsesquioxane microparticles, with diameters ranging from 0.1 to 2.0 μm, were synthesized by reacting organotrichlorosilanes in dimethylsulfoxide, used both as an oxygen-donor and a solvent, in the absence of any catalyst. Different reaction conditions were studied in order to optimize the size and shape of the organosilsesquioxane particles, including choice of solvent, use of surfactants, and addition of polystyrene.[26,106,107]

3.2.3. Organically Modified Silicates and Ceramics. NH condensation reactions are particularly useful to prepare transparent organic−inorganic hybrid materials whose properties can satisfy the requirements for photonic applications, such as a low hydroxyl content and a high degree of homogeneity.

Low-hydroxyl organically modified silicates were fabricated by a NH reaction between methyl-modified silicon halides and ter-butanol (eq 4). The sols could be doped with erbium by dissolution of anhydrous ErI_3, leading to luminescent xerogels.[108]

Methacrylate-modified chlorosilanes were either homo- or co-condensed with fluoroalkyl-modified chlorosilanes by reaction with ter-butanol. The remaining chlorosilane groups were reacted by a second alcohol treatment to obtain air-stable, highly condensed, and low OH-containing sols. The OH-content, estimated by FTIR spectroscopy, was <10% referring to materials prepared by the conventional hydrolytic process. After addition of a photoinitiator, transparent bulk materials were obtained by photopolymerization. NIR-absorbance measurements evidenced the low optical losses of bulk materials.[109] More recently, the reaction of diphenylsilanediol with 3-methacryloxypropyltrimethoxysilane at 60−100 °C in the presence of a catalyst has been used in the synthesis of photopatternable ormocers with a low silanol content.[63,110] The refractive index could be increased by co-condensation with titanium alkoxide.[111]

It is also possible to bind covalently organic groups in oxide materials by using organosilane precursors. Thus, SiO_2-TiO_2 mixed oxides comprising hydrophobic surface methyl groups were prepared in one-step by reaction of $SiCl_4$, $TiCl_4$, and $MeSiCl_3$ (or Me_3SiCl) with diisopropyl ether. These mesoporous solids turned out to be efficient catalysts in the epoxidation of alkenes with organic hydroperoxides.[89]

3.2.4. Surface Modification of Oxides by Organic Monolayers. The covalent binding of organic groups to oxide supports by reaction of surface hydroxyl with organosilanes $RSiX_3$ (X = Cl, OR, H) cannot be considered nonhydrolytic; indeed, the decrease of the monolayers density with the water content in the reaction medium indicates that hydrolysis of Si−X groups by adsorbed water is most likely involved in a first step.[112−114] On the other hand, the modification of metal oxide surfaces with phosphonic acids[115−119] does not require water as a reactant but involves the direct NH condensation of P−OH groups with surface hydroxyl groups

$$[MO_n]{-}OH + RP({=}O)(OH)_2 \rightarrow [MO_n]{-}O{-}PR({=}O)OH + H_2O \quad (15)$$

Note that in this reaction, the P−O bonds are not broken, as shown by ^{17}O NMR experiments.[120]

It has also been shown that diethyl phosphonates could be used to modify metal oxide surfaces in organic solvents at moderate temperatures.[118] The cleavage of P−O−C bonds on a metal oxide surface under mild conditions suggests that the coordination of phosphoryl oxygen atoms to Lewis acid sites on the surface assists the condensation by increasing the electrophilicity of the P atom, thus facilitating the condensation of P−O−Et groups with surface hydroxyl groups

$$[MO_n]{-}OH + RP({=}O)(OEt)_2 \rightarrow [MO_n]{-}O{-}PR({=}O)(OEt) + EtOH \quad (16)$$

3.2.5. Polymer Nanocomposites. Polymer nanocomposites, which intimately associate organic polymers and inorganic nanoparticles, have attracted considerable attention because of their high mechanical performances and their transparency, which makes them very attractive for applications in optics (contact lenses, high-refractive index materials, waveguide materials, optical coating, nonlinear optical materials, etc). However, oxide nanoparticles that arise from flame pyrolysis or aqueous syntheses cannot be easily dispersed in organic media, because of their hydrophilic character. These agglomeration problems have been shown to be circumvented by using oxide nanoparticles prepared by NH reactions: the nanaoparticles were used as obtained (SnO_2),[24] after in situ surface modification (anatase),[121] or after postsynthesis treatment with a ligand (magnetite).[52] One illustration of the potential of such approaches in the preparation of polymer nanocomposites was recently given by the excellent dispersibility of ZrO_2 nanoparticles prepared by the benzylic alcohol route in monomers, pure or in solution.[122,123] The use of vinyl group-containing ligands for the surface modification not only prevented the formation of aggregates and made the nanoparticles soluble but offered the ability to react them in a further polymerization step.[122]

The in situ formation of nanosized oxide-based fillers in polymer solutions offers an elegant alternative way. Thus, the in situ formation of hyperbranched polysiloxane macromolecules through a one-pot synthetic route based on the NH condensation reaction of tetraethoxysilane with acetic anhydride in the presence of an organotitanium catalyst[46] (eq 11) led to silica polypropylene nanocomposites with improved thermal properties.[124] Similarly hybrid materials composed of interpenetrated networks of polyaniline (PANi) and silica were prepared by using the reaction of a mixture of tetraethoxysilane (TEOS) and PANi in formic acid. This approach was based on the facts that PANi is soluble in formic acid and the acid efficiently promotes condensations leading to the polysilicate network (eqs 8−10). Transparent and monolithic hybrid glass doped with PANi has been obtained. Spectroscopic analysis in the UV−visible region as a function of the pH showed that this nanocomposite could be an efficient pH sensor.[125]

4. Control of the Morphology, Nanostructure, and Texture of Oxide-Based Materials by Using NH Condensation Reactions

4.1. Nanoparticles. The synthesis of crystalline objects with low dimensionality (0D, 1D, or 2D; i.e., quantum dots, nanowires or nanotubes, quantum wells or lamellar structures) is a challenging purpose in nanoscience, as solid-state physical properties, which depends on the length of the confined dimension, can be tuned, on a nanometer scale, between the molecular precursor and the bulk solid. Moreover, the size, shape, and size distribution of oxide nanoparticles used as fillers have dramatic effects on the properties of the resulting nanocomposites.

Actually, higher activation energies are involved by moving from aqueous to nonhydrolytic sol−gel processes, which is reflected by a drastic decrease in reaction rates and a marked trend to favor controlled crystallization and unusual crystallographic forms. Moreover the morphology of the final metal oxide strongly depends on synthesis parameters (precursor, solvent, surface modifier, etc.), providing an attractive versatility. Accordingly, the nonhydrolytic approach has recently given rise to an important renewing in low-temperature syntheses of crystalline nanoparticles with control of size and shape (spheres, rods, platelets, multipods, etc.).

Classically, the use of molecules (called surfactants and capping or passivating agents) that provide a protective

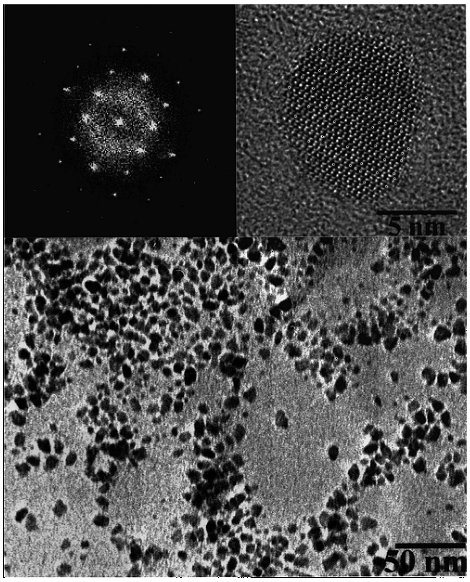

Figure 1. TEM image of titania nanoparticles derived from $TiCl_4$ and $Ti(O^iPr)_4$ in TOPO/heptadecane at 300 °C (bottom). A high-resolution TEM image of a single particle illustrates the defect free nature of these nanocrystals (top right). FFT of the particle shown verified the anatase structure and established that the image was taken down the [100] zone axis (top left). Reproduced with permission from ref 126. Copyright 1999 American Chemical Society.

organic shell to particles is required to prevent naked nanoparticles from aggregating in solution. NH sol−gel processes are particularly suitable to directly prepare organophilic nanoparticles. Actually, NH processes can be performed in the presence of surfactants (trioctylphosphine, long-chain alcohols, amines, or carboxylic acids). As in hydrolytic pathways, the surfactants can be exchanged against other ones in a postsynthesis surface modification step; alternatively, the selectivity of surfactants toward some crystal facets may favor the crystal growth in some directions. One crucial advantage of NH processes is that they can be implemented in the absence of any surfactant. Actually, in solvents such as benzylic alcohol,[7,9] which can act as a capping agent, NH sol−gel processes offer unique ways to address the challenging issue of obtaining surfactant-free nanoparticles, with nonhydroxylated surfaces, which may exhibit unique catalytic, electronic, or sintering properties.

4.1.1. Surfactant-Assisted Routes. Basically, these routes consist in the injection of a solution of molecular precursors into a hot surfactant solution (or even directly a pure surfactant). Not only size but also shape control can be achieved.

In 1999, Colvin et al. synthesized well-crystallized TiO_2 nanocrystals (Figure 1) with uniform size by alkyl halide elimination (eq 1) between titanium tetraisopropoxide and titanium tetrachloride at high-temperature in the presence of trioctylphosphine (TOPO) as a capping agent.[126] Similar reactions were used to produce ZrO_2, HfO_2 and $Hf_xZr_{1-x}O_2$ nanocrystals on the multigram scale.[127,128] The size, shape, and crystallization phase of the hafnia particles were shown to depend on both the reaction temperature and the halide. Recently, Hyeon et al. achieved the simultaneous phase- and size-controlled synthesis of TiO_2 nanorods (Figure 2) by continuous delivering of tetrachloride and tetraalkoxide titanium precursors in hot surfactant solution by means of two syringe pumps.[129] Cheon and Alivisatos et al. reported the shape evolution of titanium dioxide nanocrystals structures obtained from titanium tetraisopropoxide and titanium tetrachloride by modulation of the surface energy of the different crystallographic faces using both a non selective surfactant (TOPO) and a surface selective surfactant (lauric acid, which is known to bind strongly anatase {001} high-energy facets) (Figure 3).[130] The shape of the nanocrystals evolved from bullet to diamond, rod, and branched rod on increasing the concentration of carboxylic acid surfactant.

Cheon et al. reported a general one-pot synthesis to 1D nanocrystals of transition metal oxides ($W_{18}O_{49}$, TiO_2, Mn_3O_4, V_2O_5) (Figure 4) by reaction of metal chlorides with oleic acid and oleylamine at 350 °C.[131] Similar processes were applied to metal carboxylate and metal acetylacetonate precursors. Thus, ZnO nanocrystals with various shapes were synthesized via NH ester elimination reactions between zinc acetate and 1,12-dodecanediol.[132] The thermal decomposition of zinc acetate in organic solvents in the presence of oleic acid was reported to afford relatively monodisperse ZnO quantum rods with diameters of 2 nm and lengths in the range 40−50 nm. O'Brien and co-workers reported the synthesis of zinc oxide nanorods with a high degree of crystallinity and a narrow size distribution.[133] Monodisperse nanoparticles were synthesized by high-temperature solution-phase reaction of $Fe(acac)_3$, or $Fe(acac)_3$ and $Co(acac)_2$ or $Mn(acac)_2$, in phenyl ether with 1,2-hexadecanediol, oleic acid, and oleylamine.[134,135] Size-controlled monodisperse magnetic nanoparticles of formula MFe_2O_4 ($M = Fe, Co, Mn$) could be achieved by combining NH reaction with seed-mediated growth.[136−138] O'Brien and co-workers generalized the use of metal acetylacetonate precursors to Cr and Mn.[139] Note that the hydrophobic nanoparticles could be transformed into hydrophilic ones by adding bipolar surfactants, and aqueous nanoparticle dispersion was readily achieved, which is of interest for biomedical applications.[135,140]

Reaction between titanium tetraisopropoxide and oleic acid at 270 °C generated well-crystallized anatase TiO_2 nanorods; the diameters of the nanorods (2−3 nm) could be controlled by adding 1-hexadecylamine to the reaction mixture as a cosurfactant.[141] A mixture of titanium isopropoxide and oleic acid was used to generate carboxylate titanium complexes at 80 °C in 1-octadecene, followed by the injection of a predetermined amount of oleylamine at 260 °C to give monodisperse TiO_2 nanorods (eq 12), the lengths of which increased with the relative amount of oleylamine.[47]

4.1.2. Surfactant-Free Routes. In these routes, which generally require lower temperatures than the previous ones, the organic solvent and/or the organics formed during the reaction course act as capping agents. As mentioned above, the reaction of metal halides with benzyl alcohol was widely used to synthesize metal oxide nanoparticles. It allows a good control of the crystal growth without the use of any additional ligands. Typically, spherical anatase monodiperse nanoparticles have been synthesized by the reaction between titanium tetrachloride and benzyl alcohol at temperatures as low as 40 °C.[142] Interestingly, the size of the particles strongly depends on temperature, so that the diameter can be adjusted in the range of 4−8 nm. The effect of the relative amount

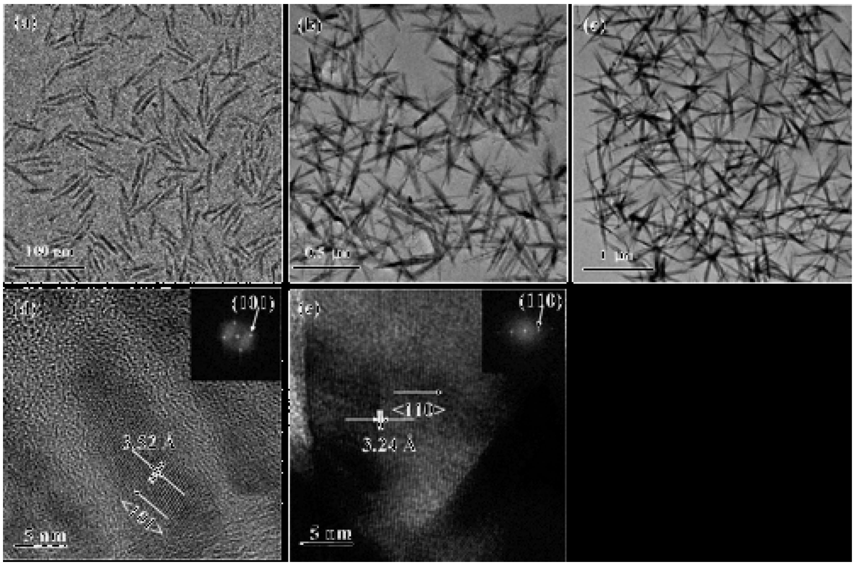

Figure 2. TEM images of TiO_2 nanorods obtained from $TiCl_4$ and $Ti(O^iPr)_4$ using an injection rate of (a) 30, (b) 2.5, and (c) 1.25 mL/h, respectively. High-resolution TEM images of (d) anatase of a and (e) rutile of c. Reproduced with permission from ref 129. Copyright 2006 American Chemical Society.

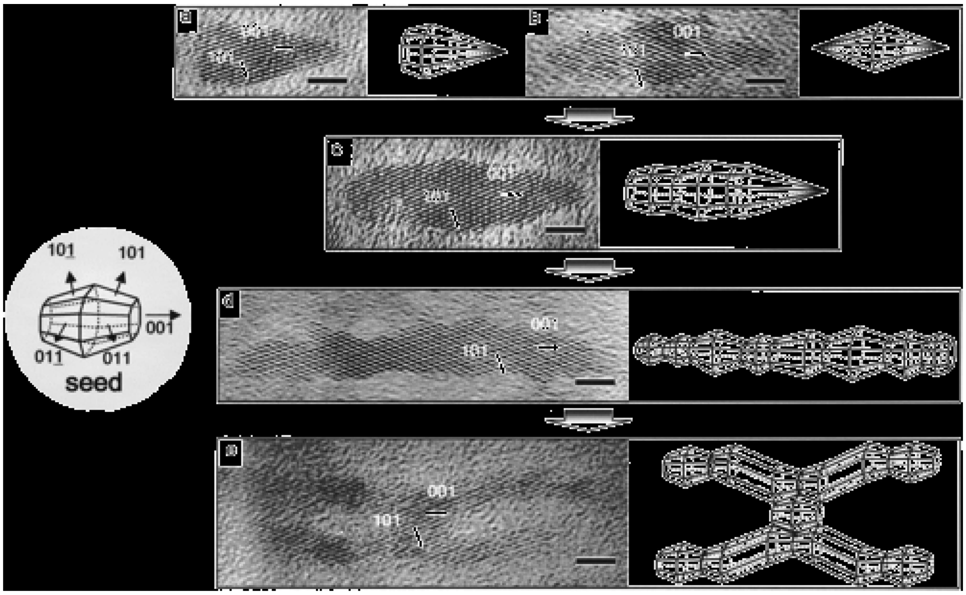

Figure 3. HRTEM analyses and simulated three-dimensional shape of TiO_2 nanostructures obtained from $TiCl_4$ and $Ti(O^iPr)_4$ in the presence of TOPO and lauric acid: (a) a bullet, (b) a diamond, (c) a short rod, (d) a long rod, and (e) a branched rod. Scale bar = 3 nm. Reproduced with permission from ref 130. Copyright 2003 American Chemical Society.

of alcohol and titanium tetrachloride has been highlighted too: lowering the concentration of $TiCl_4$ decreased to particle size. Vanadium oxide nanorods, and tungsten oxide nanoplatelets were obtained by the same route.[143]

As the presence of halide impurities in the final oxides obtained by these routes may be a drawback, alternative halide-free methods have been developed as well.[8,144] Thus, anatase nanoparticles of 5−20 nm in size were prepared through the reaction of titanium tetraisopropoxide with ketones and aldehydes under solvothermal conditions.[51] Other halide-free methods were developed by heating metal alkoxides,[25,57,145] metal acetate,[146] or metal acetylacetonates[52,146] in benzyl alcohol (Figure 5) in autoclave at 200−250 °C, leading to nanocrystals of CeO_2,[144] CoO,[146] Fe_3O_4,[52,146] HfO_2,[25] In_2O_3,[145] MnO and Mn_3O_4,[146,147] V_2O_3 and Nb_2O_5,[57] SnO_2,[145] Ta_2O_5,[25] ZnO,[146] ZrO_2.[122,123] Alternatively, Niederberger and co-workers reported the solvothermal reaction between metal acetylacetonates and benzylamine (Schemes 3, 4) as a route to nanocrystalline oxides. With the exception of the iron-based system, where a mixture of the two phases (magnetite and maghemite) was formed, only phase pure materials were obtained, γ-Ga_2O_3, zincite ZnO, and cubic In_2O_3, the particle sizes lying in the range of 15−20 nm for iron, 10−15 nm for indium, 2.5−3.5 nm for gallium, and around 20 nm for zinc (Figure 6).[53] Heating aluminum acetylacetonate in benzyl amine at 160 °C directly provided γ-alumina nanocrystals without further calcination step.[54]

The benzyl alcohol route has been extended to mixed oxides, more specifically to perovskites ($BaTiO_3$, $SrTiO_3$, $BaZrO_3$, $KNbO_3$, $NaTaO_3$, $BaSnO_3$ etc.)[6,7,55,56,148,149] It is worth noting the simultaneous use of two different metal precursors. Thus, the use of indium acetylacetonate and tin

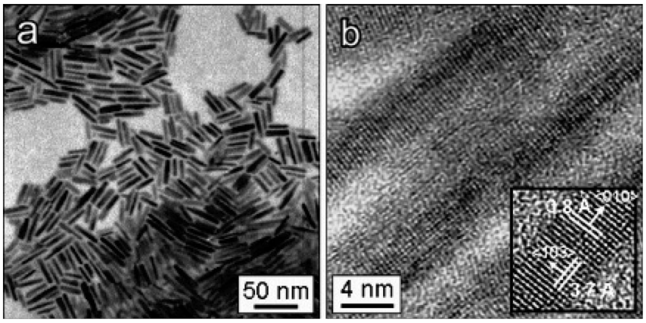

Figure 4. (a) TEM and (b) HRTEM images of tungsten oxide nanorods produced from WCl_4, oleic acid, and oleylamine at 350 °C. Inset: magnified HRTEM image showing lattice fringes of $W_{18}O_{49}$ nanorods. Reproduced with permission from ref 131. Copyright 2005 American Chemical Society.

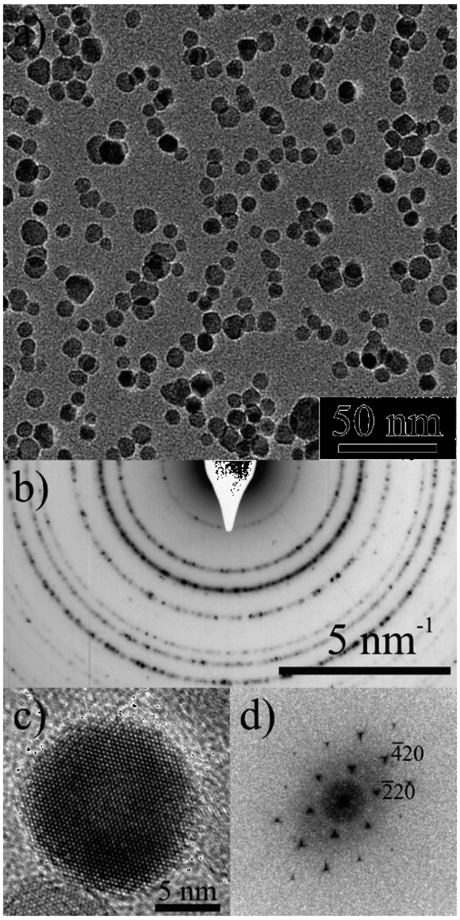

Figure 5. (a) TEM overview of magnetite particles synthesized from benzyl alcohol and iron(III) acetylacetonate at 175 °C, (b) electron diffraction of a large zone, (c) HRTEM of a unique single-crystal particle, and (d) its power spectrum. Reproduced with permission from ref 52. Copyright 2005 American Chemical Society.

tert-butoxide in the benzyl alcohol route led to nearly spherical crystalline indium tin oxide particles in the range of 5−10 nm, with tin oxide contents varying from 2 to 30 wt %.[150] Similarly $InNbO_4$ nanocrystals, with particle sizes ranging in 10−30 nm and showing a high photocatalytic activity under illumination with visible light, were synthesized by using indium acetylacetonate and niobium chloride.[151] In another work, the use of an inert solvent (anisole), which allowed to control the amount of benzyl alcohol, was shown to influence the growth, hence the morphology of nanoparticles. Thus, cobalt and manganese doped ZnO nanoparticles were prepared by reacting zinc acetate and a dopant precursor (cobalt acetate or manganese oleate) with different anisole/benzyl alcohol proportions at moderate temperature.[152]

The benzylamine route was also successfully applied to the synthesis of mixed oxides. Thus, the one-pot solvothermal reaction of metal acetylacetonates with benzylamine led to $ZnGa_2O_4$ nanocrystals with a mean size of about 7 nm, which could easily be dispersed in chloroform; interestingly the resulting stable colloidal solution showed an intense blue emission under UV light.[153]

It is worth mentioning here the “glycothermal” syntheses developed by Inoue et al. to synthesize nanoparticles of crystallized mixed oxides by thermal decomposition of metal precursors such as salts, alkoxides, acetylacetonates, and acetates in glycols or aminoalcohols (typically in 1,4-butanediol at 200−300 °C).[154,155]

4.2. Mesoscopic Self-Assemblies of Crystallites. As a general feature, oxide nanoparticules stemming from NH processes are coated with organic groups related to either surfactant additives or to the oxygen donor (e.g., benzyl alcohol). These organic groups have been shown to contribute not only to the control of size and shape as capping agents, but also to the self-assembly into mesoscopic arrangements and hybrid superstructures through bonding interactions (e.g., Van der Waals or $\pi-\pi$ interactions).[12,156] Thus, following controlled evaporation from nonpolar solvents, nanoparticles stemming from the thermal decomposition of precursors in the presence of surfactants were observed to self-assemble into uniform stacking[133] two-dimensional arrays and three-dimensional[136,157] superlattices.[5] In some cases, the presence of organics on the crystal faces has been shown to be able to move the crystal growth mechanism from classical nucleation-and-growth process to oriented attachment process. Oriented attachment process refers to the spontaneous self-organization of primary nanoparticles, so that they share a common crystallographic orientation, before forming an iso-oriented crystal upon fusion.[158] The driving force of the fusion is provided by the minimization of surface energy associated with junction of adjacent particles through coherent planar interface.

Such processes are known to be involved in the formation of anisotropic nanoparticles. Thus, Zitoun et al. reported an affordable, high-yield, shape-controlled synthesis of MnO multipod crystalline nanoparticles, in which $Mn(oleate)_2$ and oleic acid were heated in trioctylamine at 320 °C (Figure 7).[159] The exclusive formation of 2−6 pod single crystals was ascribed to an oriented attachment mechanism, which relied on the formation of chainlike aggregates due to an induced dipole−dipole interaction. According to this mechanism, each MnO primary crystallite would have six equivalent facets, which would be able to assemble along six directions.

Monitoring the indium tin oxide (ITO) crystallization during solvothermal synthesis in benzyl alcohol shed light on nonclassical crystallization mechanisms that involve intermediate hybrid superstructures. A two-step process was shown to be involved. First, the formation of an intermediary

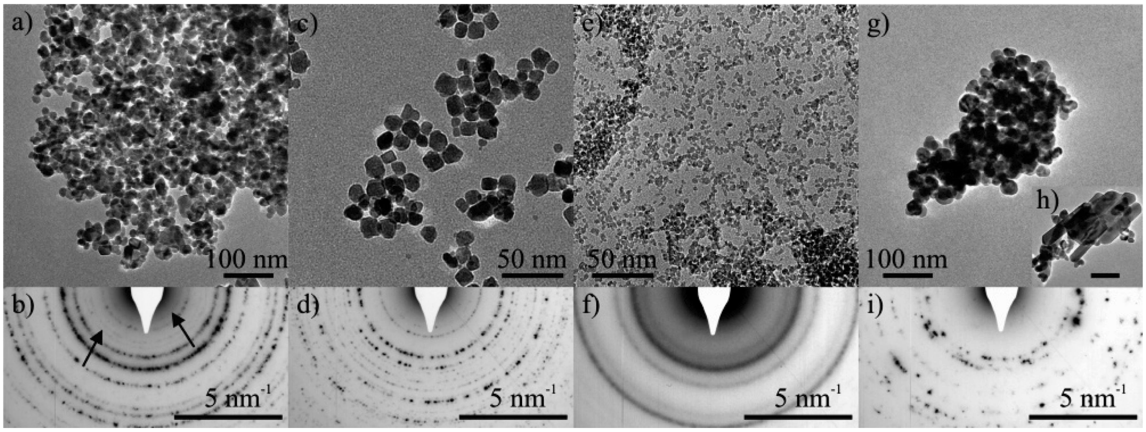

Figure 6. TEM overview images of (a) iron oxide, (c) indium oxide, (e) gallium oxide, and (g, h) zinc oxide nanoparticles (scale bar 100 nm) obtained by reaction of acetylacetonates with benzylamine at 200 °C and their respective SAED patterns (b, d, f, and i). Reproduced with permission from ref 53. Copyright 2005 American Chemical Society.

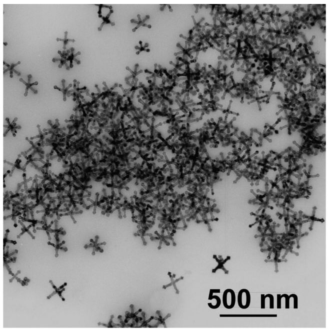

Figure 7. TEM overview image of an assembly of MnO multipods produced from manganese oleate and oleic acid in trioctylamine at 320 °C (courtesy of D. Zitoun et al.).

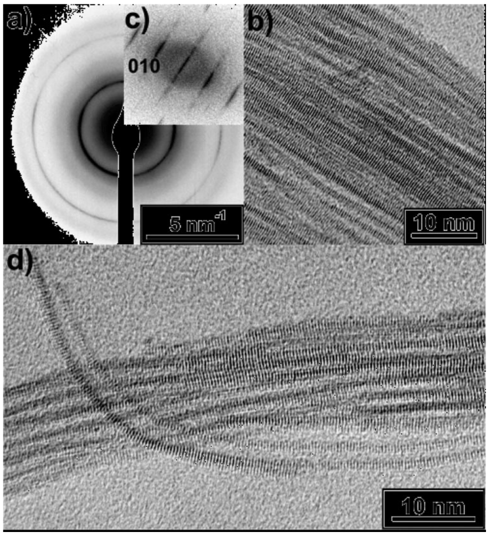

Figure 8. Tungsten oxide nanowires obtained by reaction of WCl_6 and benzyl alcohol in the presence of the bioligand deferoxamine mesylate; (a) SAED pattern, (b) HRTEM image, (c) power spectrum of the HRTEM shown in (b), and (d) HRTEM image of linear and curved nanowires. Reproduced with permission from ref 163. Copyright 2005 American Chemical Society.

phase consisting of aligned nanocrystallites (3−6 nm) embedded in an organic matrix, followed by the transformation into the bixbyite structure with larger crystallites (10−12 nm) accompanied by the disappearance of both the organic phase and the superstructure.[160]

Actually, the benzyl alcohol route has been shown to favor the formation of self-assembled oxide nanoparticles. One noticeable feature of this route is that benzaldehyde, benzoate and benzoic acid are able to form in situ through Oppenauer oxidation reactions (see section 2.6), and to coordinate onto the incipient oxide species, acting both as structure directing agents and molecular "assemblers" between crystallites. The synthesis of tungsten oxide nanoparticles by the benzyl alcohol route well-illustrates the versatility of NH solvothermal reactions and the role of organics (precursor, solvent and byproduct). The reaction of tungsten isopropoxide with benzyl alcohol led to WO_3 nanobundles, which consisted of self-assembled nanowires.[161] The uniform distance between the nanowires was shown to result from an ordered supramolecular arrangement of intercalated benzaldehyde molecules adsorbed to the oxide surface. Removing the adsorbed benzaldehyde molecules by addition of formamide resulted in individual nanowires with a uniform diameter of about 1 nm. On the other hand, the reaction of tungsten chloride in benzyl alcohol led to nanoplatelets consisting of a large number of crystallographically almost perfectly aligned primary crystallites, just a few nanometers in size. In 4-*tert*-butylbenzyl alcohol, the self-organization reached two hierarchical levels, where the stacked platelets formed nanocolumns perfectly arranged over a length scale of up to 10 μm, these stacks being in turn assembled laterally into polydisperse bundles.[162] When deferoxamine mesylate was used as a bioligating additive in benzyl alcohol, long nanowires of $W_{18}O_{49}$ (diameter 1.3 nm; aspect ratio higher than 500) organized into bundles (Figure 8) were obtained.[163]

The benzylamine route was shown to lead to highly ordered hybrid structures as well. As a matter of fact, the solvothermal reaction of titanium isopropoxide in benzyl amine led to complex structures consisting of anatase nanoplatelets that were stacked in a lamellar fashion with a small organic layer in between.[164] Benzylamine, which was identified as the sole species in the organic layer between the nanocrystals, was responsible for both shape control and alignment of the inorganic crystals.

The above-mentioned in situ formation of benzoate and benzoic acid, which are able to bind strongly to the forming inorganic material during solvothermal reactions in benzyl

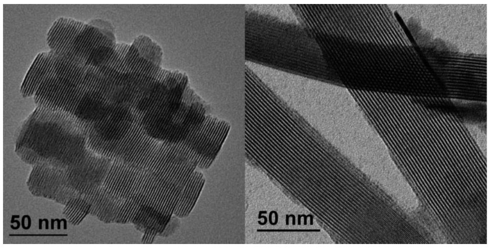

Figure 9. TEM images of hybrid nanostructures: neodynium oxide-based benzoate (left) and biphenolate (right) hybrids (courtesy of N. Pinna et al.).

alcohol, also provides a simple one-step way to stable, nanostructured organic−inorganic hybrid materials.[4,12] The key point is then the ability of the incipient oxide material to catalyze the formation of benzoate and benzoic acid. Thus, reaction of Ln(III) isopropoxides (Ln = Y, Gd, Sm, Nd) with benzyl alcohol (or even 4-biphenylmethanol), for a few days in an autoclave at 250−300 °C, led to highly ordered 2-D hybrid nanostructures, which consisted of alternating thin layer (about 0.6 nm) of crystalline lanthanide oxide and benzoate (or biphenolate) molecules (Figure 9).[58,165] When the inorganic layers were doped with optically active lanthanide ions they showed outstanding emission properties in the green (Tb^{3+}), red (Eu^{3+}), and near IR (Nd^{3+}).[166] Energy transfer processes from the phenyl ring of the benzoate groups to the lanthanide ions (antenna effect) were evidenced. These hybrid materials present significant advantages compared to standard phosphors, such as higher radiance and luminance values, the possibility to tune the emission chromaticity by varying the excitation wavelength without loosing the radiance, and a much larger excitation range (250−350 nm and 300−500 nm for the Eu^{3+} and Nd^{3+} doped nanohybrids, respectively) with the maximum shifted toward the red.[165,167]

4.3. Porous Materials. *4.3.1. With Micelle Templating.* There is a strong interest in mesoporous oxides, especially in the catalysis area. Most strategies developed to prepare these materials involve the addition of organic structure-directing agents (templates). Typically, the cooperative self−assembly of surfactants and polycondensed oxide species is able to induce more or less ordered mesostructures, which are kept in the bulk solids after elimination (by calcination or washing) of the template. Micelle or mesophase formation from charged or neutral surfactants is based on hydrophobic/hydrophilic interactions; accordingly, most procedures involve the use of water.

However, the general method proposed by Stucky and coworkers to prepare ordered mesoporous oxides (TiO_2, ZrO_2, Nb_2O_5, Ta_2O_5, Al_2O_3, SnO_2, HfO_2, WO_3, etc.) is based on the reaction of metal chlorides with alcohols in the presence of amphiphilic block copolymers as structure-directing agents.[168,169] Nonhydrolytic reactions are likely involved even though water (arising from atmospheric moisture and from the solvent) is present in the process.

The nonhydrolytic thermolytic decomposition of terbutyloxy(siloxy) derivatives in solution in the presence of block copolymers led to mesoporous, multicomponent oxides or phosphates (ZrO_2−$4SiO_2$, Ta_2O_5−$6SiO_2$, Fe_2O_3, $6SiO_2$, and $AlPO_4$) with high surface areas, wormhole-like pore structure, and narrow pore size distributions.[69] However, in this case, water was also produced along with isobutylene.

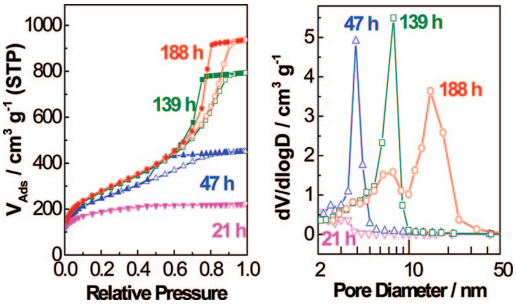

Figure 10. N_2 adsorption−desorption isotherm at 77 K (left) and pore-size distribution (right) of calcined SiO_2−TiO_2 xerogels (Si/Ti = 10) prepared from chloride precursors and diisopropylether at 110 °C for different reaction times (after ref 73).

Stable sols of cassiterite nanocrystals were obtained in THF from the simple reaction of $SnCl_4$ with benzyl alcohol. Addition of a polybutadiene-block-poly(ethylene oxide) and evaporation of THF induced the self-assembly of the nanocrystals and the block copolymer micelles. Tin oxide with highly ordered mesoporosity was obtained after calcination.[24] Similarly the polymer directed assembly of crystalline cerium oxide nanoparticle sols led to highly ordered mesoporous powders.[170]

4.3.2. Without Micelle Templating. As in conventional sol−gel processing, the first template is the liquid phase (solvent plus byproducts) trapped in the gel and pore volume may be generated by the removal of this liquid phase trapped in the gel. The porosity of solids stemming from NH sol−gel markedly depends on the synthesis parameters, such as concentration, metal precursor, oxygen donor, and catalyst.[18] NH tin oxide and tin−aluminum mixed oxide aerogels with high porosity (90%) were prepared using low-temperature supercritical drying of CO_2 exchanged gels.[78] However nonhydrolytic gels, which are generally highly condensed compared to the hydrolytic ones, are able to withstand the capillary stresses generated by solvent evaporation and to keep high mesoporosity after drying, without using supercritical conditions. Thus, silicas with stable "aerogel-like" structure (surface area of 720 m^2/g and pore volume of 1.4 cm^3/ g), could be achieved via the formic acid route (eqs 8−10) by using an ionic liquid as solvent, which was simply washed off with a polar solvent.[37]

Homogeneous mesoporous silica−titania xerogels with specific surface areas ranging from 450 to 1200 $m^2\ g^{-1}$ and pore volumes ranging from 0.24 to 2.4 $cm^3\ g^{-1}$ were also obtained by alkyl halide elimination (eq 1) without any template or resorting to supercritical drying.[74,96] The porosity of these NH xerogels was shown to be governed by the volume fraction of liquid phase and by the degree of condensation, which permits adjustment of the texture simply by changing the volume of solvent, the reaction time (Figure 10), or the reaction temperature. It must be noted that using conventional sol−gel routes, only microporous silica−titania xerogels could be prepared.

In an original nonsolution way, alumina foams with exceptionally high porosity ranging from 94 to 99% were generated by simple heat treatment of crystals of complex

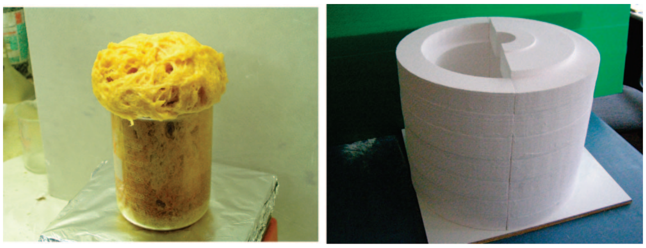

Figure 11. Alumina foams produced from $AlCl_3.Pr^i_2O$, with elimination of Pr^iCl. Fresh foam (left) and commercial bare module (right) (courtesy of G. Grader).

$AlCl_3.Pr^i_2O$, leading to the elimination of Pr^iCl (eq 2).[171,172] First, $AlO_xCl_y(OPr^i)_z$ species formed, which dissolved in liquid Pr^iCl. Accordingly, the boiling point of the solution was raised above the boiling point of pure Pr^iCl. Polycondensation then progressed in the liquid until a critical polymer size was reached, whereupon a phase separation into polymer rich and solvent rich regions occurred. Because the expelled solvent was suddenly above its boiling point, bubbles formed instantly. Foam stabilization took place as a result of gelation in the polymer rich regions. The foams consisted of closed cells with diameters in the 50−300 μm range, with cell walls about 1−2 μm thick. Surface area measurements showed that the cell walls contained nanometer-sized pores. The cellular structure was retained at 1500 °C with only a small shrinkage in the foam dimensions.[81,171] These aluma foams are marketed as ultralight fiber-free thermal insulating materials in Israel by Cellaris ltd (Figure 11).[173]

4.4. Inorganic Monolayers and Thin Films. The grafting of monolayers or submonolayers of metal oxide species by reaction of metal alkoxides with hydroxylated surfaces in the absence of water has been extensively used in the preparation of heterogeneous catalysts.[64,174−176] More recently, catalysts with well-isolated sites were prepared by reacting an hydroxylated silica support with a solution of tris-terbutyloxysiloxy ($-OSi(O^tBu)_3$) derivatives of titanium or iron with elimination of $HOSi(O^tBu)_3$.[65,100] Nonhydrolytic surface condensation was also used to deposit a heterobinuclear V/Ti complex at the surface of hydroxylated silica by successive reactions with vapors of $VOCl_3$ and $Ti(O-^iPr)_4$.[177]

Atomic layer deposition (ALD) is an elegant method for the formation of highly conformal thin films structures; this process is based on alternate self-limited surface reactions.[178] ALD of metal oxides involves a metallic precursor (typically chlorides, alkoxides or alkyl derivatives) and an oxygen donor, usually water.

Brei et al. were the first to employ NH condensation for ALD of boron phosphate and titanium silicate by pulsing alternately chlorides and alkoxides (Figure 12) with elimination of alkyl chloride (eq 2).[179,180]

Later, Ritala and co-workers demonstrated the versatility of this NH route, which appears quite general for the production of oxide (Al_2O_3, Ta_2O_5, TiO_2)[181−183] and mixed oxide thin films (Si/Ti, Zr/Si, Hf/Si, Al/Ti, Hf/Ti, Zr/Ti, Al/Zr, Hf/Al).[67,180,181,184−188] Other oxygen donors, such as alcohols and di-iso-propyl ether have also been used for the ALD of alumina or titania films from metal chlorides (eqs 2 and 3).[188−191]

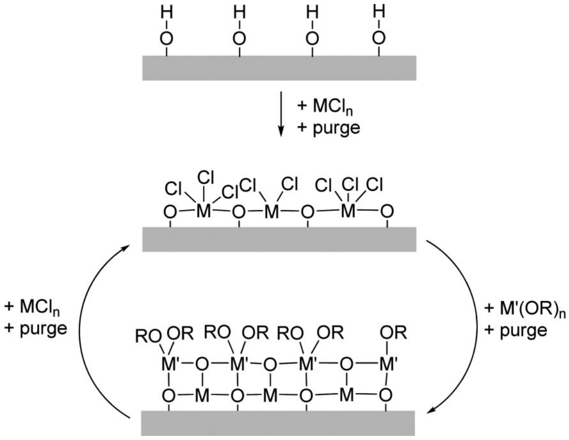

Figure 12. Schematic representation of the nonhydrolytic atomic layer deposition of a mixed metal oxide film from chloride and alkoxide precursors.

Quite recently, Rauwel and co-workers[31] deposited TiO_2 and HfO_2 from metal akoxide precursors using carboxylic acids oxygen donors. The deposition is attributed to the exchange of alkoxide ligands by carboxylate groups (eq 8) with elimination of alcohol, followed in the next pulse by nonhydrolytic condensation involving ester elimination (eq 7). The main drawback of NH condensations is their low reaction rates, compared to the hydrolysis condensation of metal chlorides or alkyl metal precursors. ALD is inherently a slow technique and the reactivity requirements are completely different from that of sol−gel: in ALD, typical pulse lengths are around 1 s, whereas in sol−gel processing, reaction times at 110 °C range from a few hours to several days. This low reactivity led ALD researchers to use high deposition temperatures (150−500 °C). However, above ca. 300 °C the thermal decomposition of alkoxide becomes significant. Thus, in a mechanistic study of the ALD of $Zr_xTi_yO_z$ from $Ti(O^iPr)_4$ and $ZrCl_4$, Rahtu et al. found that at 300 °C about 80% of the oxide growth involved the expected ^iPrCl elimination, and about 20% involved elimination of propene and HCl.[67] The deposition of silicates with very high growth per cycle from tris(tert-butoxy)silanol and $AlMe_3$[192] or metal chlorides[193] or from $Si(O^nBu)_4$ and $Zr(NEt_2)_4$ most likely involves thermal decomposition reactions catalyzed by metallic species.[194]

The main anticipated advantage in ALD of metal oxide films using NH reactions is related to the low oxidative character of the oxygen donors compared to water, H_2O_2 or O_3, which permitted the deposition of an Al_2O_3[183] (Figure 13) or of a silicate[194,195] film on silicon without an interfacial silicon oxide layer.

A nonhydrolytic surface sol−gel process resembling ALD has been proposed for the layer-by-layer modification of powdered mesoporous silica with titania.[196] This method is based on successive reactions of the support with $Ti(O^iPr)_4$ and $TiCl_4$ at 110 °C in anhydrous chloroform. The excess of reactant is not removed between each step, which probably accounts for the high growth rate (compared to ALD) of the titania film (0.5−0.8 nm per layer).

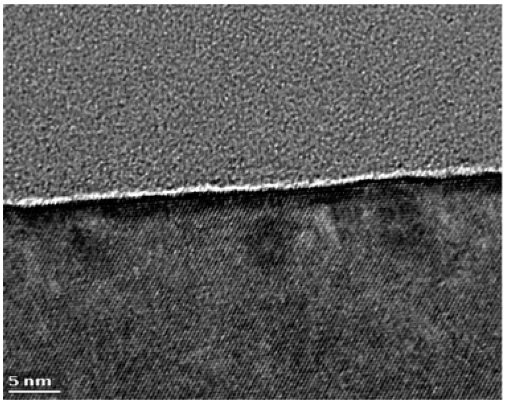

Figure 13. High-resolution transmission electron microscope image of the interface between a silicon substrate and Al_2O_3 film grown at 300 °C. The $AlCl_3$ and $Al(O^iPr)_3$ pulse lengths were 0.2 and 0.5 s, respectively. Reproduced with permission from ref 183. Copyright 2002 The Royal Society of Chemistry.

5. Conclusions

NH condensation reactions broaden the scope of sol−gel processing and solvothermal synthesis. Especially, they open the possibility of working up in organic solvents, in unusual nonaqueous media such as perfluorinated solvents, ionic liquids, supercritical CO_2, pure surfactants, or even in the absence of any solvent. They open the possibility of using molecular precursors cheaper and more available than metal alkoxides, such as metal halides, acetates, and acetyacetonates. They give access to metastable phases, low-hydroxyl oxides and high-performance hybrid inorganic−organic nanocomposites. They make it possible to implement simpler one-step syntheses, without additives, organic templates or capping agents. Thus, in the case of mixed oxides, one-step processes permit us to simultaneously control not only the compositional homogeneity, but also the surface functionality (e.g., by introducing hydrophobic groups) and the porosity, without the use of any reactivity modifier, templating agent or further supercritical drying step, which is of considerable interest in catalysis. The trend of NH processes to decrease reaction rates and to favor controlled crystallization, has given rise recently to important developments in low-temperature syntheses of highly crystalline nanoparticles, with controlled size and shape and outstanding monodispersity. Particularly, they offer unique ways to obtain particles with surfactant-free nonhydroxylated surfaces, which again is of considerable interest in catalysis, sensing, and photonics. They open access to stable colloids in nonaqueous media and hydrophobic nanofillers, the application of which has just emerged in the field of polymer nanocomposites. In relation to the presence of organics on the surface, oxide nanoparticles stemming from NH processes are prone to self-assemble into mesoscopic superstructures organized on a length scale ranging from a few nanometers to several micrometers. This self-assembly has been applied to the synthesis of nanostructured hybrid organic−inorganic materials with outstanding properties; they open fascinating prospects to biomimetic processes. NH condensation reactions were also successfully applied to surface modification, and particularly to atomic layer deposition, with the advantage of milder oxidative conditions. The field of application of NH condensation reactions is evolving rapidly and should continue to give rise to innovative developments in material sciences.

References

(1) Vioux, A.; Mutin, P. H. *Handbook of Sol−Gel Science & Technology*; Kluwer Academic Publishers: Norwell, MA, 2005; Vol. 1, p 621.
(2) Vioux, A. *Chem. Mater.* **1997**, *9*, 2292.
(3) Hay, J. N.; Raval, H. M. *Chem. Mater.* **2001**, *13*, 3396.
(4) Pinna, N. *J. Mater. Chem.* **2007**, *17*, 2769.
(5) Jun, Y.-W.; Choi, J.-S.; Cheon, J. *Angew. Chem., Int. Ed.* **2006**, *45*, 3414.
(6) Niederberger, M.; Garnweitner, G.; Pinna, N.; Neri, G. *Prog. Solid State Chem.* **2006**, *33*, 59.
(7) Garnweitner, G.; Niederberger, M. *J. Am. Ceram. Soc.* **2006**, *89*, 1801.
(8) Niederberger, M.; Garnweitner, G. *Chem.−Eur. J.* **2006**, *12*, 7282.
(9) Niederberger, M. *Acc. Chem. Res.* **2007**, *40*, 793.
(10) Niederberger, M.; Garnweitner, G.; Ba, J.; Polleux, J.; Pinna, N *Int. J. Nanotechnol.* **2007**, *4*, 263.
(11) Pinna, N.; Niederberger, M. *Angew. Chem., Int. Ed.* **2008**, *47*, 5292.
(12) Garnweitner, G.; Niederberger, M. *J. Mater. Chem.* **2008**, *18*, 1171.
(13) Zhang, L.; Garnweitner, G.; Djerdj, I.; Antonietti, M.; Niederberger, M *Chem. Asian J.* **2008**, *3*, 746.
(14) Gerrard, W.; Woodhead, A. H. *J. Chem. Soc.* **1951**, 519.
(15) Corriu, R.; Leclercq, D.; Lefevre, P.; Mutin, P. H.; Vioux, A. *Chem. Mater.* **1992**, *4*, 961.
(16) Corriu, R. J. P.; Leclercq, D.; Lefevre, P.; Mutin, P. H.; Vioux, A. *J. Mater. Chem.* **1992**, *2*, 673.
(17) Corriu, R. J. P.; Leclercq, D.; Lefevre, P.; Mutin, P. H.; Vioux, A. *J. Non-Cryst. Solids* **1992**, *146*, 301.
(18) Bourget, L.; Corriu, R. J. P.; Leclercq, D.; Mutin, P. H.; Vioux, A. *J. Non-Cryst. Solids* **1998**, *242*, 81.
(19) Andrianainarivelo, M.; Corriu, R.; Leclercq, D.; Mutin, P. H.; Vioux, A. *J. Mater. Chem.* **1996**, *6*, 1665.
(20) Corriu, R. J. P.; LeClercq, D.; Lefevre, P.; Mutin, P. H.; Vioux, A. *J. Non-Cryst. Solids* **1992**, *151*, 272.
(21) Turova, N. Y. ; Turevskaya, E. P.; Kessler, V., G.; Yanovskaya, M., I. *Oxoalkoxides*; Kluwer Academic: Norwell, MA, 2002, p. 69.
(22) Bourget, L.; Mutin, P. H.; Vioux, A.; Frances, M. *J. Polym. Sci., Part A* **1998**, *36*, 2415.
(23) Deng, Z.-X.; Wang, C.; Li, Y.-D. *J. Am. Ceram. Soc.* **2002**, *85*, 2837.
(24) Ba, J.; Polleux, J.; Antonietti, M.; Niederberger, M. *Adv. Mater.* **2005**, *17*, 2509.
(25) Pinna, N.; Garnweitner, G.; Antonietti, M.; Niederberger, M. *Adv. Mater.* **2004**, *16*, 2196.
(26) Arkhireeva, A.; Hay, J. N.; Manzano, M. *Chem. Mater.* **2005**, *17*, 875.
(27) Jansen, M.; Guenther, E. *Chem. Mater.* **1995**, *7*, 2110.
(28) Caruso, J.; Hampden-Smith, M. J. *J. Sol−Gel Sci. Technol.* **1997**, *8*, 35.
(29) Stathatos, E.; Lianos, P.; Lavrencic-Stangar, U.; Orel, B. *Adv. Mater.* **2002**, *14*, 354.
(30) Wang, C.; Deng, Z.-X.; Li, Y.-D. *Inorg. Chem.* **2001**, *40*, 5210.
(31) Rauwel, E.; Clavel, G.; Willinger, M.-G.; Rauwel, P.; Pinna, N. *Angew. Chem., Int. Ed.* **2008**, *47*, 3592.
(32) Sharp, K. G. *J. Sol−-Gel Sci. Technol.* **1994**, *2*, 35.
(33) Sharp, K. G. *Adv. Mater.* **1998**, *10*, 1243.
(34) Khimich, N. N.; Venzel, B. I.; Koptelova, L. A. *Dokl. Phys. Chem.* **2002**, *385*, 201.
(35) Brankova, T.; Bekiari, V.; Lianos, P. *Chem. Mater.* **2003**, *15*, 1855.
(36) Sharp, K. G. *J. Mater. Chem.* **2005**, *15*, 3812.
(37) Dai, S.; Ju, Y. H.; Gao, H. J.; Lin, J. S.; Pennycook, S. J.; Barnes, C. E. *Chem. Commun.* **2000**, *3*, 243.
(38) Neouze, M.-A.; Le Bideau, J.; Leroux, F.; Vioux, A. *Chem. Commun.* **2005**, 1082.
(39) Sui, R.; Rizkalla, A. S.; Charpentier, P. A. *J. Phys. Chem. B* **2004**, *108*, 11886.
(40) Green, W. H.; Le, K. P.; Grey, J.; Au, T. T.; Sailor, M. J. *Science* **1997**, *276*, 1826.
(41) Sui, R.; Rizkalla, A. S.; Charpentier, P. A. *Langmuir* **2005**, *21*, 6150.
(42) Sui, R.; Rizkalla, A. S.; Charpentier, P. A. *Langmuir* **2006**, *22*, 4390.
(43) Arnal, P.; Corriu, R. J. P.; Leclercq, D.; Mutin, P. H.; Vioux, A. *J. Mater. Chem.* **1996**, *6*, 1925.
(44) Fujiwara, M.; Wessel, H.; Park, H. S.; Roesky, H. W. *Chem. Mater.* **2002**, *14*, 4975.
(45) Guo, G.; Whitesell, J. K.; Fox, M. A. *J. Phys. Chem. B* **2005**, *109*, 18781.
(46) Zhu, X.; Jaumann, M.; Peter, K.; Möller, M.; Melian, C.; Adams-Buda, A.; Demco, D. E.; Bluemich, B. *Macromolecules* **2006**, *39*, 1701.
(47) Zhang, Z.; Zhong, X.; Liu, S.; Li, D.; Han, M. *Angew. Chem., Int. Ed.* **2005**, *44*, 3466.
(48) Cozzoli, P. D.; Curri, M. L.; Agostiano, A.; Leo, G.; Lomascolo, M. *J. Phys. Chem. B* **2003**, *107*, 4756.
(49) Steunou, N.; Ribot, F.; Boubekeur, K.; Maquet, J.; Sanchez, C. *New J. Chem.* **1999**, *23*, 1079.
(50) Steunou, N.; Sanchez, C.; Forster, S.; Goltner, C.; Antonietti, M.; Florian, P. *Ceram. Trans.* **2001**, *123*, 49.
(51) Garnweitner, G.; Antonietti, M.; Niederberger, M. *Chem. Commun.* **2005**, 397.
(52) Pinna, N.; Grancharov, S.; Beato, P.; Bonville, P.; Antonietti, M.; Niederberger, M. *Chem. Mater.* **2005**, *17*, 3044.

(53) Pinna, N.; Garnweitner, G.; Antonietti, M.; Niederberger, M. *J. Am. Chem. Soc.* **2005**, *127*, 5608.

(54) Zhou, S.; Antonietti, M.; Niederberger, M. *Small* **2007**, *3*, 763.

(55) Niederberger, M.; Garnweitner, G.; Pinna, N.; Antonietti, M. *J. Am. Chem. Soc.* **2004**, *126*, 9120.

(56) Niederberger, M.; Garnweitner, G.; Pinna, N.; Antonietti, M. *J. Am. Chem. Soc.* **2004**, *126*, 9120.

(57) Pinna, N.; Antonietti, M.; Niederberger, M. *Colloids Surf., A* **2004**, *250*, 211.

(58) Pinna, N.; Garnweitner, G.; Beato, P.; Niederberger, M.; Antonietti, M. *Small* **2005**, *1*, 112.

(59) Zha, C.; Atkins, G. R.; Masters, A. F. *J. Sol−Gel Sci. Technol.* **1998**, *13*, 103.

(60) Guerrero, G.; Mutin, P. H.; Vioux, A. *Chem. Mater.* **2000**, *12*, 1268.

(61) Wipfelder, E.; Hoehn, K. *Angew. Makromol. Chem.* **1994**, *218*, 111.

(62) Alder, K. I.; Sherrington, D. C. *J. Mater. Chem.* **2000**, *10*, 1103.

(63) Houbertz, R.; Froehlich, L.; Popall, M.; Streppel, U.; Dannberg, P.; Braeuer, A.; Serbin, J.; Chichkov, B. N. *Adv. Eng. Mater.* **2003**, *5*, 551.

(64) Kijenski, J.; Baiker, A.; Glinski, M.; Dollenmeier, P.; Wokaun, A. *J. Catal.* **1986**, *101*, 1.

(65) Jarupatrakorn, J.; Tilley, T. D. *J. Am. Chem. Soc.* **2002**, *124*, 8380.

(66) Kominami, H.; Kohno, M.; Matsunaga, Y.; Kera, Y. *J. Am. Ceram. Soc.* **2001**, *84*, 1178.

(67) Rahtu, A.; Ritala, M. *Langmuir* **2002**, *18*, 10046.

(68) Terry, K. W.; Tilley, T. D. *Chem. Mater.* **1991**, *3*, 1001.

(69) Kriesel, J. W.; Sander, M. S.; Tilley, T. D. *Adv. Mater.* **2001**, *13*, 331.

(70) Fujdala, K. L.; Tilley, T. D. *Chem. Mater.* **2002**, *14*, 1376.

(71) Lugmair, C. G.; Fujdala, K. L.; Tilley, T. D. *Chem. Mater.* **2002**, *14*, 888.

(72) Brutchey, R. L.; Lugmair, C. G.; Schebaum, L. O.; Tilley, T. D. *J. Catal.* **2005**, *229*, 72.

(73) Hay, J. N.; Raval, H. M. *J. Mater. Chem.* **1998**, *8*, 1233.

(74) Lafond, V.; Mutin, P. H.; Vioux, A. *Chem. Mater.* **2004**, *16*, 5380.

(75) Acosta, S.; Corriu, R.; Leclercq, D.; Mutin, P. H.; Vioux, A. *J. Sol−Gel Sci. Technol.* **1994**, *2*, 25.

(76) Acosta, S.; Corriu, R. J. P.; Leclercq, D.; Hubert Mutin, P.; Vioux, A. *Mater. Res. Soc. Symp. Proc.* **1994**, *346*, 345.

(77) Janackovic, D.; Orlovic, A.; Skala, D.; Drmanic, S.; Kostic-Gvozdenovic, L. K.; Jokanovic, V.; Uskokovic, D. *Nanostruct. Mater.* **1999**, *12*, 147.

(78) Harreld, J. H.; Sakamoto, J.; Dunn, B. *J. Power Sources* **2003**, *115*, 19.

(79) Andrianainarivelo, M.; Corriu, R. J. P.; Leclercq, D.; Mutin, P. H.; Vioux, A. *Chem. Mater.* **1997**, *9*, 1098.

(80) Linacero, R.; Rojas-Cervantes, M. L.; Lopez-Gonzalez, J. D. D. *J. Mater. Sci.* **2000**, *35*, 3269.

(81) Mann, M.; Shter, G. E.; Grader, G. S. *J. Mater. Res.* **2002**, *17*, 831.

(82) Andrianainarivelo, M.; Corriu, R. J. P.; Leclercq, D.; Mutin, P. H.; Vioux, A. *J. Mater. Chem.* **1997**, *7*, 279.

(83) Xu, J.; Lind, C.; Wilkinson, A. P.; Pattanaik, S. *Chem. Mater.* **2000**, *12*, 3347.

(84) Wilkinson, A. P.; Lind, C.; Pattanaik, S. *Chem. Mater.* **1999**, *11*, 101.

(85) Gates, S. D.; Colin, J. A.; Lind, C. *J. Mater. Chem.* **2006**, *16*, 4214.

(86) Barbieri, F.; Cauzzi, D.; De Smet, F.; Devillers, M.; Moggi, P.; Predieri, G.; Ruiz, P. *Catal. Today* **2000**, *61*, 353.

(87) Huang, W.; Tang, X.; Felner, I.; Koltypin, Y.; Gedanken, A. *Mater. Res. Bull.* **2002**, *37*, 1721.

(88) Popa, A. F.; Mutin, P. H.; Vioux, A.; Delahay, G.; Coq, B. *Chem. Commun.* **2004**, 2214.

(89) Mutin, P. H.; Popa, A. F.; Vioux, A.; Delahay, G.; Coq, B. *Appl. Catal., B* **2006**, *69*, 49.

(90) Caetano, B. L.; Rocha, L. A.; Molina, E.; Rocha, Z. N.; Ricci, G.; Calefi, P. S.; de Lima, O. J.; Mello, C.; Nassar, E. J.; Ciuffi, K. J. *Appl. Catal., A* **2006**, *311*, 122.

(91) Di Vona, M. L.; Traversa, E.; Licoccia, S. *Chem. Mater.* **2001**, *13*, 141.

(92) Moggi, P.; Predieri, G.; Cauzzi, D.; Devillers, M.; Ruiz, P.; Morselli, S.; Ligabue, O. *Stud. Surf. Sci. Catal.* **2002**, *143*, 149.

(93) Moggi, P.; Devillers, M.; Ruiz, P.; Predieri, G.; Cauzzi, D.; Morselli, S.; Ligabue, O. *Catal. Today* **2003**, *81*, 77.

(94) Mutin, H.; Lafond, V.; Vioux, A. Patent EP1685139, 2005.

(95) Lorret, O.; Lafond, V.; Mutin, P. H.; Vioux, A. *Chem. Mater.* **2006**, *18*, 4707.

(96) Cojocariu, A. M.; Mutin, P. H.; Dumitriu, E.; Fajula, F.; Vioux, A.; Hulea, V. *Chem. Commun.* **2008**, 5357.

(97) Lafond, V.; Mutin, P. H.; Vioux, A. *J. Mol. Catal. A* **2002**, *182−183*, 81.

(98) Rulkens, R.; Male, J. L.; Terry, K. W.; Olthof, B.; Khodakov, A.; Bell, A. T.; Iglesia, E.; Tilley, T. D. *Chem. Mater.* **1999**, *11*, 2966.

(99) Coles, M. P.; Lugmair, C. G.; Terry, K. W.; Tilley, T. D. *Chem. Mater.* **2000**, *12*, 122.

(100) Nozaki, C.; Lugmair, C. G.; Bell, A. T.; Tilley, T. D. *J. Am. Chem. Soc.* **2002**, *124*, 13194.

(101) de Lima, O. J.; de Aguirre, D. P.; de Oliveira, D. C.; da Silva, M. A.; Mello, C.; Leite, C. A. P.; Sacco, H. C.; Ciuffi, K. J. *J. Mater. Chem.* **2001**, *11*, 2476.

(102) Mac Leod, T. C. O.; Guedes, D. F. C.; Lelo, M. R.; Rocha, R. A.; Caetano, B. L.; Ciuffi, K. J.; Assis, M. D. *J. Mol. Catal. A* **2006**, *259*, 319.

(103) Caiut, J. M. A.; Nakagaki, S.; De Lima, O. J.; Mello, C.; Leite, C. A. P.; Nassar, E. J.; Ciuffi, K. J.; Sacco, H. C. *J. Sol−Gel Sci. Technol.* **2003**, *28*, 57.

(104) Apperley, D.; Hay, J. N.; Raval, H. M. *Chem. Mater.* **2002**, *14*, 983.

(105) Hay, J. N.; Porter, D.; Raval, H. M. *J. Mater. Chem.* **2000**, *10*, 1811.

(106) Arkhireeva, A.; Hay, J. N.; Lane, J. M.; Manzano, M.; Masters, H.; Oware, W.; Shaw, S. J. *J. Sol−Gel Sci. Technol.* **2004**, *31*, 31.

(107) Arkhireeva, A.; Hay, J. N. *Polym. Polym. Composites* **2004**, *12*, 101.

(108) Yuh, S.-K.; Bescher, E. P.; Babonneau, F.; Mackenzie, J. D. *Mater. Res. Soc. Symp. Proc.* **1994**, *346*, 803.

(109) Mennig, M.; Zahnhausen, M.; Schmidt, H. *Proc. SPIE Int. Soc. Opt. Eng.* **1998**, *3469*, 68.

(110) Buestrich, R.; Kahlenberg, F.; Popall, M.; Dannberg, P.; Muller-Fiedler, R.; Rosch, O. *J. Sol−Gel Sci. Technol.* **2001**, *20*, 181.

(111) Kim, W.-S.; Yoon, K. B.; Bae, B.-S. *J. Mater. Chem.* **2005**, *15*, 4535.

(112) Ulman, A. *Chem. Rev.* **1996**, *96*, 1533.

(113) Tripp, C. P.; Hair, M. L. *Langmuir* **1995**, *11*, 1215.

(114) Fadeev, A. Y.; McCarthy, T. J. *J. Am. Chem. Soc.* **1999**, *121*, 12184.

(115) Gao, W.; Dickinson, L.; Grozinger, C.; Morin, F. G.; Reven, L. *Langmuir* **1996**, *12*, 6429.

(116) Helmy, R.; Fadeev, A. Y. *Langmuir* **2002**, *18*, 8924.

(117) Gawalt, E. S.; Avaltroni, M. J.; Danahy, M. P.; Silverman, B. M.; Hanson, E. L.; Midwood, K. S.; Schwarzbauer, J. E.; Schwartz, J. *Langmuir* **2003**, *19*, 200.

(118) (a) Guerrero, G.; Mutin, P. H.; Vioux, A. *Chem. Mater.* **2001**, *13*, 4367.
(b) Guerrero, G.; Mutin, P. H; Vioux, A. *J. Mater. Chem.* **2001**, *11*, 3161.

(119) Mutin, P. H.; Guerrero, G.; Vioux, A. *J. Mater. Chem.* **2005**, *15*, 3761.

(120) Lafond, V.; Gervais, C.; Maquet, J.; Prochnow, D.; Babonneau, F.; Mutin, P. H. *Chem. Mater.* **2003**, *15*, 4098.

(121) Niederberger, M.; Garnweitner, G.; Krumeich, F.; Nesper, R.; Coelfen, H.; Antonietti, M. *Chem. Mater.* **2004**, *16*, 1202.

(122) Zhou, S.; Garnweitner, G.; Niederberger, M.; Antonietti, M. *Langmuir* **2007**, *23*, 9178.

(123) Garnweitner, G.; Goldenberg, L. M.; Sakhno, O. V.; Antonietti, M.; Niederberger, M.; Stumpe, J. *Small* **2007**, *3*, 1626.

(124) Zhu, X.; Peter, K.; Moeller, M.; Melian, C.; Adams-Buda, A.; Demco, D. E. *Polym. Prep.* **2006**, *47*, 1133.

(125) de Azevedo, W. M.; Brondani, D. J. *J. Non-Cryst. Solids* **2001**, *296*, 224.

(126) Trentler, T. J.; Denler, T. E.; Bertone, J. F.; Agrawal, A.; Colvin, V. L. *J. Am. Chem. Soc.* **1999**, *121*, 1613.

(127) Joo, J.; Yu, T.; Kim, Y. W.; Park, H. M.; Wu, F.; Zhang, J. Z.; Hyeon, T. *J. Am. Chem. Soc.* **2003**, *125*, 6553.

(128) Tang, J.; Fabbri, J.; Robinson, R. D.; Zhu, Y.; Herman, I. P.; Steigerwald, M. L.; Brus, L. E. *Chem. Mater.* **2004**, *16*, 1336.

(129) Koo, B.; Park, J.; Kim, Y.; Choi, S.-H.; Sung, Y.-E.; Hyeon, T. *J. Phys. Chem. B* **2006**, *110*, 24318.

(130) Jun, Y. W.; Casula, M. F.; Sim, J.-H.; Kim, S. Y.; Cheon, J.; Alivisatos, A. P. *J. Am. Chem. Soc.* **2003**, *125*, 15981.

(131) Seo, J.-W.; Jun, Y.-W.; Ko, S. J.; Cheon, J. *J. Phys. Chem. B* **2005**, *109*, 5389.

(132) Joo, J.; Kwon, S. G.; Yu, J. H.; Hyeon, T. *Adv. Mater.* **2005**, *17*, 1873.

(133) Yin, M.; Gu, Y.; Kuskovsky, I. L.; Andelman, T.; Zhu, Y.; Neumark, G. F.; O'Brien, S. *J. Am. Chem. Soc.* **2004**, *126*, 6206.

(134) Sun, S.; Zeng, H. *J. Am. Chem. Soc.* **2002**, *124*, 8204.

(135) Sun, S.; Zeng, H.; Robinson, D. B.; Raoux, S.; Rice, P. M.; Wang, S. X.; Li, G. *J. Am. Chem. Soc.* **2004**, *126*, 273.

(136) Zeng, H.; Rice Philip, M.; Wang Shan, X.; Sun, S. *J. Am. Chem. Soc.* **2004**, *126*, 11458.

(137) Song, Q.; Zhang, Z. J. *J. Am. Chem. Soc.* **2004**, *126*, 6164.

(138) Park, J.; Lee, E.; Hwang, N.-M.; Kang, M.; Kim, S. C.; Hwang, Y.; Park, J.-G.; Noh, H.-J.; Kim, J.-Y.; Park, J.-H.; Hyeon, T. *Angew. Chem., Int. Ed.* **2005**, *44*, 2872.

(139) Andelman, T.; Gong, Y.; Polking, M.; Yin, M.; Kuskovsky, I.; Neumark, G.; O'Brien, S. *J. Phys. Chem. B* **2005**, *109*, 14314.

(140) Xie, J.; Peng, S.; Brower, N.; Pourmand, N.; Wang, S. X.; Sun, S. *Pure Appl. Chem.* **2006**, *78*, 1003.

(141) Joo, J.; Kwon, S. G.; Yu, T.; Cho, M.; Lee, J.; Yoon, J.; Hyeon, T. *J. Phys. Chem. B* **2005**, *109*, 15297.

(142) Niederberger, M.; Bartl, M. H.; Stucky, G. D. *Chem. Mater.* **2002**, *14*, 4364.

(143) Niederberger, M.; Bartl, M. H.; Stucky, G. D. *J. Am. Chem. Soc.* **2002**, *124*, 13642.

(144) Niederberger, M.; Garnweitner, G.; Buha, J.; Polleux, J.; Ba, J.; Pinna, N. *J. Sol−Gel Sci. Technol.* **2006**, *40*, 259.

(145) Pinna, N.; Neri, G.; Antonietti, M.; Niederberger, M. *Angew. Chem., Int. Ed.* **2004**, *43*, 4345.

(146) Bilecka, I.; Djerdj, I.; Niederberger, M. *Chem. Commun.* **2008**, 886.

(147) Djerdj, I.; Arcon, D.; Jaglicic, Z.; Niederberger, M. *J. Phys. Chem. C* **2007**, *111*, 3614.

(148) Niederberger, M.; Pinna, N.; Polleux, J.; Antonietti, M. *Angew. Chem., Int. Ed.* **2004**, *43*, 2270.

(149) Niederberger, M.; Antonietti, M. Patent WO2005021426, 2005.

(150) Ba, J.; Fattakhova Rohlfing, D.; Feldhoff, A.; Brezesinski, T.; Djerdj, I.; Wark, M.; Niederberger, M. *Chem. Mater.* **2006**, *18*, 2848.

(151) Zhang, L.; Djerdj, I.; Cao, M.; Antonietti, M.; Niederberger, M. *Adv. Mater.* **2007**, *19*, 2083.

(152) Clavel, G.; Willinger, M.-G.; Zitoun, D.; Pinna, N. *Adv. Funct. Mater.* **2007**, *17*, 3159.

(153) Cao, M.; Djerdj, I.; Antonietti, M.; Niederberger, M. *Chem. Mater.* **2007**, *19*, 5830.

(154) Inoue, M. *J. Phys.: Condens. Matter* **2004**, *16*, S1291.

(155) Takahashi, M.; Inoue, N.; Takeguchi, T.; Iwamoto, S.; Inoue, M.; Watanabe, T. *J. Am. Ceram. Soc.* **2006**, *89*, 2158.

(156) Antonietti, M.; Niederberger, M.; Smarsly, B. *Dalton Trans.* **2008**, 18.

(157) Yin, M.; Chen, Z.; Deegan, B.; O'Brien, S. *J. Mater. Res.* **2007**, *22*, 1987.
(158) Niederberger, M.; Coelfen, H. *Phys. Chem. Chem. Phys.* **2006**, *8*, 3271.
(159) Zitoun, D.; Pinna, N.; Frolet, N.; Belin, C. *J. Am. Chem. Soc.* **2005**, *127*, 15034.
(160) Ba, J.; Feldhoff, A.; Rohlfing, D. F.; Wark, M.; Antonietti, M.; Niederberger, M. *Small* **2007**, *3*, 310.
(161) Polleux, J.; Gurlo, A.; Barsan, N.; Weimar, U.; Antonietti, M.; Niederberger, M. *Angew. Chem., Int. Ed.* **2006**, *45*, 261.
(162) Polleux, J.; Antonietti, M.; Niederberger, M. *J. Mater. Chem.* **2006**, *16*, 3969.
(163) Polleux, J.; Pinna, N.; Antonietti, M.; Niederberger, M. *J. Am. Chem. Soc.* **2005**, *127*, 15595.
(164) Garnweitner, G.; Tsedev, N.; Dierke, H.; Niederberger, M. *Eur. J. Inorg. Chem.* **2008**, 890.
(165) Karmaoui, M.; Mafra, L.; Sa Ferreira, R. A.; Rocha, J.; Carlos, L. D.; Pinna, N. *J. Phys. Chem. C* **2007**, *111*, 2539.
(166) Karmaoui, M.; Sa Ferreira, R. A.; Mane, A. T.; Carlos, L. D.; Pinna, N. *Chem. Mater.* **2006**, *18*, 4493.
(167) Ferreira, R. A. S.; Karmaoui, M.; Nobre, S. S.; Carlos, L. D.; Pinna, N. *Chem. Phys. Chem.* **2006**, *7*, 2215.
(168) Yang, P. D.; Zhao, D. Y.; Margolese, D. I.; Chmelka, B. F.; Stucky, G. D. *Nature* **1998**, *396*, 152.
(169) Yang, P. D.; Zhao, D. Y.; Margolese, D. I.; Chmelka, B. F.; Stucky, G. D. *Chem. Mater.* **1999**, *11*, 2813.
(170) Deshpande, A. S.; Pinna, N.; Smarsly, B.; Antonietti, M.; Niederberger, M. *Small* **2005**, *1*, 313.
(171) Grader, G. S.; De Hazan, Y.; Shter, G. E. *Ceram. Trans.* **1998**, *95*, 161.
(172) Grader, G. S.; Shter, G. E.; De Hazan, Y. *J. Mater. Res.* **1999**, *14*, 1485.
(173) Grader, G.; Shter, G.; Dehazan, Y. Patent WO9951541, 1999.
(174) Fernandez, A.; Leyrer, J.; Gonzalez-Elipe, A. R.; Munuera, G.; Knoezinger, H. *J. Catal.* **1988**, *112*, 489.
(175) Schraml-Marth, M.; Wokaun, A.; Baiker, A. *J. Catal.* **1990**, *124*, 86.
(176) Castillo, R.; Koch, B.; Ruiz, P.; Delmon, B.; Castillo, R.; Koch, B.; Ruiz, P.; Delmon, B., *Scientific Bases for the Preparation of Heterogeneous Catalysts. Preparation of Catalysts VI*; Elsevier: Amsterdam, 1995.
(177) Rice, G. L.; Scott, S. L. *Chem. Mater.* **1998**, *10*, 620.
(178) Leskela, M.; Ritala, M. *Angew. Chem., Int. Ed.* **2003**, *42*, 5548.
(179) Brei, V. V.; Gulyanitsky, N. E.; Kaspersky, V. A.; Chuiko, A. A. *Dokl. Akad. Nauk Ukr.* **1991**, 112.
(180) Brei, V. V.; Kaspersky, V. A.; Gulyanitskaya, N. U. *React. Kinet. Catal. Lett.* **1993**, *50*, 415.
(181) Ritala, M.; Kukli, K.; Rahtu, A.; Raisanen, P. I.; Leskela, M.; Sajavaara, T.; Keinonen, J. *Science* **2000**, *288*, 319.
(182) Kukli, K.; Ritala, M.; Leskelae, M. *Chem. Mater.* **2000**, *12*, 1914.
(183) Raeisaenen, P. I.; Ritala, M.; Leskelae, M. *J. Mater. Chem.* **2002**, *12*, 1415.
(184) Rahtu, A.; Ritala, M.; Leskelae, M. *Chem. Mater.* **2001**, *13*, 1528.
(185) Kim, W.-K.; Kang, S.-W.; Rhee, S.-W.; Lee, N.-I.; Lee, J.-H.; Kang, H.-K. *J. Vac. Sci. Technol., A* **2002**, *20*, 2096.
(186) Kim, W.-K.; Rhee, S.-W.; Lee, N.-I.; Lee, J.-H.; Kang, H.-K. *J. Vac. Sci. Technol., A* **2004**, *22*, 1285.
(187) Kukli, K.; Ritala, M.; Leskelae, M.; Sajavaara, T.; Keinonen, J.; Hegde, R. I.; Gilmer, D. C.; Tobin, P. J. *J. Electrochem. Soc.* **2004**, *151*, F98.
(188) Prince, K. E.; Evans, P. J.; Triani, G.; Zhang, Z.; Bartlett, J. *Surf. Interface Anal.* **2006**, *38*, 1692.
(189) Hiltunen, L.; Kattelus, H.; Leskela, M.; Makela, M.; Niinisto, L.; Nykanen, E.; Soininen, P.; Tiitta, M. *Mater. Chem. Phys.* **1991**, *28*, 379.
(190) Tiitta, M.; Nykanen, E.; Soininen, P.; Niinisto, L.; Leskela, M.; Lappalainen, R. *Mater. Res. Bull.* **1998**, *33*, 1315.
(191) Evans, P. J.; Mutin, P. H.; Triani, G.; Prince, K. E.; Bartlett, J. R. *Surf. Interface Anal.* **2006**, *38*, 740.
(192) Hausmann, D.; Becker, J.; Wang, S.; Gordon, R. G. *Science* **2002**, *298*, 402.
(193) He, W.; Solanki, R.; Conley, J. F., Jr.; Ono, Y. *J. Appl. Phys.* **2003**, *94*, 3657.
(194) Kim, J.; Yong, K. *Electrochem. Solid-State Lett.* **2004**, *7*, F35.
(195) Kim, J.; Yong, K. *J. Cryst. Growth* **2004**, *263*, 442.
(196) Yan, W.; Mahurin, S. M.; Overbury, S. H.; Dai, S. *Chem. Mater.* **2005**, *17*, 1923.

CM802348C